Heliyon 10 (2024) e38291

Contents lists available at ScienceDirect

Heliyon

journal homepage: www.cell.com/heliyon

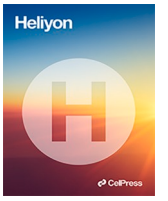

Research article

Evaluation of soil erosion in the Changhua River Basin on Hainan Island based on the Chinese soil loss equation model

Xiwen Li [a,b,**,1], Zhenqi Song [b,1], Yuefeng Lu [b,c,d,*], Baofeng Weng [e], Jing Li [b], Yanru Liu [b], Zhenli Wang [e], You Gou [f]

[a] Haikou Marine Geological Survey Center, China Geological Survey, Haikou, China
[b] School of Civil Engineering and Geomatics, Shandong University of Technology, Zibo, China
[c] National Center of Technology Innovation for Comprehensive Utilization of Saline-Alkali Land, Dongying, China
[d] State Key Laboratory of Resources and Environmental Information System, Institute of Geographical Sciences and Natural Resources Research, Chinese Academy of Sciences, Beijing, China
[e] Zhejiang Academy of Surveying and Mapping, Hangzhou, China
[f] Guiyang Baiyun District Municipal Development and Construction Co.,Ltd., Guiyang, China

ARTICLE INFO

Keywords:
China soil erosion model
Soil erosion
Spatial interpolation
Superposition analysis
Temporal and spatial change characteristics

ABSTRACT

Soil erosion is one of the most serious ecological and environmental problems facing southern China. The Changhua River Basin on Hainan Island is affected by soil erosion, which is causing the soil environment to become more fragile. Compared with the Revised Soil Erosion Equation (RUSLE), the Chinese Soil Loss Equation (CSLE) is based on a large amount of Chinese local data and research results, which more accurately reflect the actual situation of soil erosion in China and therefore have better accuracy and applicability in the Chinese region. By combining GIS and RS technologies, this study establishes the CSLE model of the Changhua River Basin, quantifies the soil erosion data via image elements from 2020 to 2022 using the spatial interpolation method, classifies the erosion intensity, and analyzes the spatial and temporal change characteristics of soil erosion. The statistical results show that, during the period from 2020 to 2022, the area of slight erosion in the Changhua River Basin increased by 553.25 km^2, with a rate of change of 15.83 %, and the areas of mild erosion, moderate erosion, intense erosion, very intense erosion, and severe erosion decreased by 446.42 km^2, 64.4 km^2, 25.73 km^2, 11.25 km^2, and 5.45 km^2, respectively, with rates of change of −31.05 %, −30.08 %, −36.58 %, −18.02 %, and −13.85 %, respectively. Slight erosion is defined as soil erosion less than the permissible soil loss and is not regarded as soil erosion, and the other erosion intensities showed a yearly decreasing trend, indicating that the soil erosion control was effective during this three-year period. In the work of soil and water conservation, it is especially necessary to determine the main factors influencing soil erosion and predict the areas that may be prone to such erosion. Therefore, on the basis of establishing a characteristic model using land use type, slope and soil type, and through superposition analysis, we obtained the spatial and temporal change characteristics of soil erosion. The research results are as follows: (1) slight erosion is mainly concentrated in forested areas, and forested land has a better capacity for soil and water conservation; (2) mild, moderate, and strong erosion mainly occur in cultivated areas and areas with a slope of 0–5°; (3) areas of built land and

* Corresponding author. School of Civil Engineering and Geomatics, Shandong University of Technology, Zibo, China.
** Corresponding author. Haikou Marine Geological Survey Center, China Geological Survey, Haikou, China.
E-mail addresses: lxw1818168@163.com (X. Li), yflu@sdut.edu.cn (Y. Lu).
[1] These authors contributed equally to this work.

https://doi.org/10.1016/j.heliyon.2024.e38291
Received 6 May 2024; Received in revised form 19 September 2024; Accepted 20 September 2024
Available online 21 September 2024

areas with a slope of 8°–15° are more prone to intense erosion, although they cover a smaller area; (4) when the slope is greater than 15°, the overlap range with the forest area is larger and the slope is no longer the main factor leading to soil erosion. Thus, it can be seen that forest land significantly reduces the impact of soil erosion. (5) among the different soil types, Technosol, Ferralsol and Fluvisol all have less than 55 per cent uneroded area and are generally less erosion-resistant, while Lixisol and Acrisol are relatively more susceptible to a high degree of erosion hazard (Extremely strong erosion, severe erosion).

1. Introduction

Soil erosion is a natural phenomenon in which soil is denuded, transported, and deposited under the joint action of external forces such as wind, water, and gravity [1,2]. Soil erosion is one of the most serious forms of soil degradation worldwide, and ecological problems have become increasingly prominent as a result of increased soil erosion due to irrational human exploitation of natural resources [3,4]. It poses a serious threat to the sustainability of terrestrial ecosystems and the productive capacity of agriculture [5]. Over the past 50 years, soil erosion has resulted in the disappearance of nearly one-third of the world's arable land; this land continues to disappear at a rate of more than 10 million hectares per year [6,7]. Therefore, soil erosion has become a major environmental problem that needs to be solved as a matter of urgency [8].

Currently, scholars around the world mainly utilize the following models to calculate the soil erosion modulus and monitor soil erosion: the Universal Soil Loss Model (USLE) [9], the Revised Universal Soil Loss Model (RUSLE) [10], the Water Erosion Prediction Project (WEPP) model [11], and the Limburg Soil Erosion Model (LISEM) [12]. Among them, USLE is a generalized soil erosion equation pioneered and developed by the United States Department of Agriculture (USDA) by combining the soil loss rate, rainfall, runoff, soil properties, topography, vegetation cover, and land information [13,14]. It is widely used because of its simple structure and easy access to parameters; in 1997, Renard et al. revised and improved it, and further proposed the Revised Universal Soil Loss Equation (RUSLE), which improved its accuracy to a certain extent [15]. The WEPP model resulted from a research project conducted by the U.S. Department of Agriculture (USDA) in the 1990s, and the WEPP model was developed by the USDA. In the 1990s, it was developed and refined by USDA scientists and researchers to predict soil water erosion processes by simulating rainfall, runoff, and soil erosion processes [16,17]. The Limburg Soil Erosion Model (LISEM) was developed by researchers at the Agricultural University of Wageningen in the Netherlands in the 1980s, and it is mainly used to simulate and evaluate the soil erosion process. It is widely used in the fields of water resource management and land-use planning [18,19]. In the field of soil and water conservation, Chinese scholars have established runoff plots in various regions to obtain a large amount of observational data, which can be used to modify the USLE model and establish a soil erosion model that is applicable to the Chinese region. For example, Cai Qiangguo et al. [20] established a sub-rainfall erosion and sand production model, which integrates rainfall infiltration, runoff dispersion, gravity erosion, and sediment transport processes. Cai Chongfa et al. [21] established a geographic database of typical small watersheds and utilized the USLE model to predict the amount of soil erosion in the small watersheds. Jiang Zhongshen et al. [22] corrected the erosion impact coefficients of shallow gullies and established a soil loss model for calculating the inter-gully rainfall. Liu Baoyuan et al. [23] established a soil loss model for the calculation of inter-gully rainfall and an erosion model. Liu Baoyuan et al. [23] proposed biological measure factor (B), an engineering measure factor (E), and a tillage measure factor (T) by comprehensively considering the soil erosion situation and soil and water conservation measures in China, combining a large amount of runoff plot data and factors such as the land-use type, precipitation, and vegetation, etc. They further improved these factors based on RUSLE and finally constructed a soil erosion model that is more applicable to China (CSLE). With the further development of remote sensing technology, larger numbers of scholars are combining GIS tools with the Chinese soil erosion model (CSLE) [24], applying it to different cities and watersheds to quantitatively analyze the spatial and temporal changes in soil erosion characteristics.

In addition, China is currently one of the countries most seriously affected by soil erosion in the world. In particular, hydraulic erosion is more serious in the south where there is more precipitation compared to the north of China [25,26]. Soil erosion is particularly serious in the Changhua River basin in Hainan Province, which is located in the southernmost part of China. Due to the relatively weak research on remote sensing monitoring technology, the comprehensive soil and water conservation management in the Changhua River Basin in the past could only rely on the intuitive interpretation of remote sensing images and field surveys to obtain soil and water erosion data. For example, Pan Xianzhang et al. [27] completed the field calibration of soil erosion maps based on 3S integration technology, i.e., using off-road vehicles as platforms, applying GPS real-time positioning technology, and carrying out field soil erosion disaster investigation with remote sensing images under the support of GISdesktop system. Liang Yin's team [28] analyzed the evolution of soil erosion in the southern red soil area by using data from three remote sensing surveys of the Ministry of Water Resources, combined with field sampling surveys.The above studies show that Chinese experts are beginning to gradually integrate remote sensing technology with soil erosion monitoring, but there are still problems of high cost and low efficiency, as well as difficulties in systematically and comprehensively grading soil erosion across the entire watershed. Therefore, an effective soil erosion monitoring method is urgently needed to improve the efficiency of soil and water conservation work in the Changhua River Basin.

For this reason, this study combines GIS, RS technology, and the geospatial information of the Changhua River Basin to calculate each erosion factor and construct the CSLE model. It also completes the grading and mapping of the soil erosion intensity in the Changhua River Basin using spatial interpolation, map algebra, and superposition analysis. Finally, by analyzing the erosion data and their spatial and temporal change characteristics, the main factors leading to the occurrence of soil erosion were identified.

Additionally, the areas that may be prone to soil erosion in the future were predicted, with a view to providing a scientific basis for the implementation of environmental management and soil and water conservation work in the Changhua River Basin. At the same time, we aimed to promote the study of soil erosion in subtropical regions and other areas characterized by heavy precipitation.

2. Materials and methods

2.1. Research area

The Changhua River Basin is located in the northwestern part of Hainan Island, China, with a latitude and longitude range between 108°37′-109°46′E and 18°35′N-19°31′N, respectively, covering a total area of about 5320 km^2. It is thus one of the largest inland river basins on Hainan Island [29,30]. The landforms of the Changhua River Basin are complex and diverse, dominated by mountains and hills, with small and scattered plains. The topography exhibits obvious changes in undulation, with an overall inclined trend of "high in the southeast and low in the northwest", and a gradual rise in plain terraces, terraces, hills, and mountains from the northwest to the southeast [31–33]. From the northwestern plain with an elevation of 30m to the southeastern mountains with an elevation of 1654m, a geographic environment with large topographic ups and downs is formed. In addition, the Changhua River Basin, which has an average elevation of 463 m, has a tropical monsoon oceanic climate, with an average annual temperature ranging from 24.1 °C to 25.1 °C. The natural vegetation is mainly dominated by evergreen broad-leaved forests, and the main land-use types include forest land, grassland, and cropland and building land [34–36]. According to the relevant statistics, the average annual precipitation in this watershed is 1353.7 mm, and more than 90 % of this precipitation is concentrated in the summer; this precipitation distribution pattern has a serious impact on soil erosion [37]. Compared with other plain areas with high precipitation such as Guangdong Province and Hainan Province in China, the Changhua River Basin has more complex geomorphological features (mountains, hills, and plains) and more diverse land-use types, which are geographic factors that have a significant impact on soil erosion processes [38]. Moreover, the Changhua River Basin has a different social development context, such as soil and water conservation policies and soil and water conservation management measures carried out since 2019. Therefore, choosing the Changhua River Basin as the study area not only helps to study the spatial distribution characteristics of soil erosion in southern China, but also further analyses in-depth the formation mechanism of soil erosion disasters and the main factors leading to the occurrence of disasters based on the attributes of different geographical features [39,40].

Moreover, due to the changes in agriculture and forestry and the irrational expansion of urban construction, the land-use pattern in the Changhua River Basin is imbalanced; this results in a decrease in the soil retention capacity of the basin, leading to the occurrence of soil erosion. By combining high-resolution satellite remote sensing images, DEM data, and land-use-type data from 2020 to 2022, we

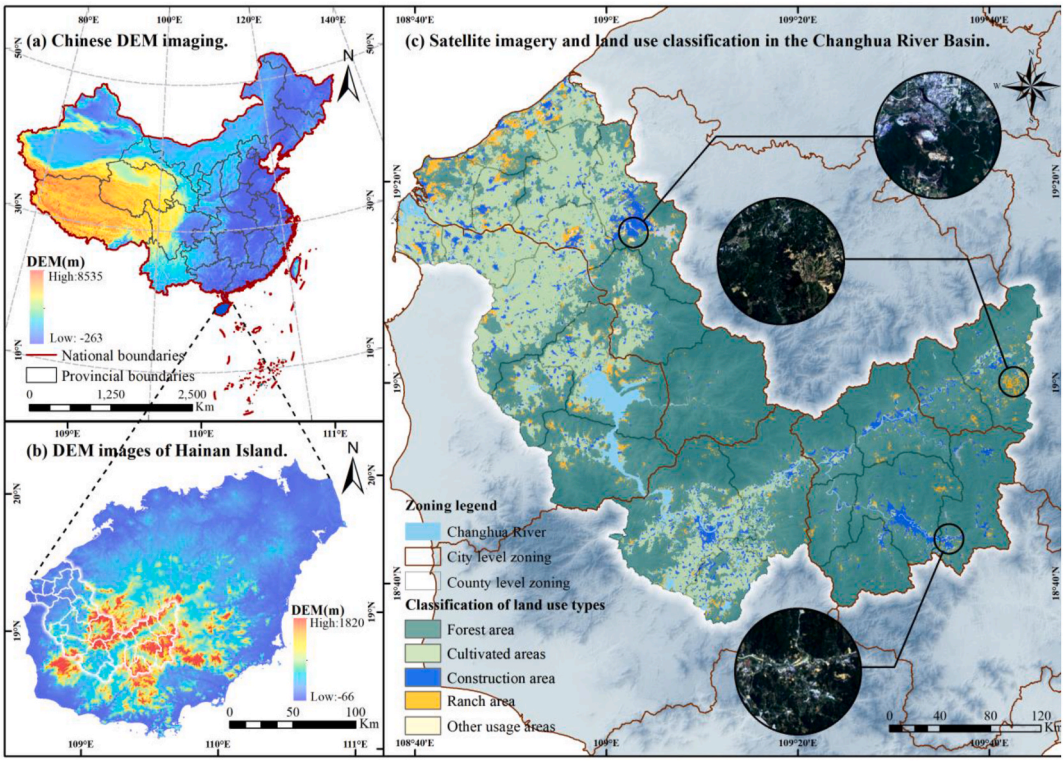

Fig. 1. Overview map of the study area.

constructed an overview map of the study area, as shown in Fig. 1.

2.2. Research data

2.2.1. Data presentation

The main data utilized in this paper are as follows: the administrative district vector data of the Changhua River Basin on Hainan Island; Sentinel-2 satellite remote sensing image data and DEM data d erived from the Geospatial Data Cloud website (http://www.gscloud.cn/); soil data from the U.S. Geological Survey (USGS, http://www.usgs.gov/); Landsat 8 data from the official website of the Google Earth Engine (GEE); meteorological data from the center of the National Meteorological Administration of China (NMAC); and annual and monthly rainfall monitoring data from the Changhua River Basin and its surrounding areas on Hainan Island. In addition, as in the Changhua Creek watershed, land use type data have a greater impact on the results of subsequent erosion calculations. Therefore, 300 sampling points (covering all land use types) were randomly set up in the study area, and the land use attributes of the points were collected through field surveys to verify the accuracy of the raw data. Based on the survey data, the interpolation algorithm was used to correct the abnormal or blank areas in the original data. Subsequently, based on the metre-level high-resolution satellite remote sensing images, it was superimposed and analyzed with the once-corrected land use type data. Through visual interpretation, the boundary range of each land-use type was further corrected in terms of image elements, in order to ultimately ensure the accuracy of the land-use type data [41,42]. Lists of the specific data and preprocessing methods used are shown in Table 1.

2.2.2. Data pre-processing methods

Data preprocessing of the satellite remote sensing images was first carried out by performing image preprocessing for each band in the Lantsat8 high-resolution satellite remote sensing images by using the radiometric calibration tool of the ENVI 5.3.1 (64-bit) software, selecting the interleaved output type as BLL and the output data type as Float in order to complete the radiometric calibration. Atmospheric correction was then performed using the FLAASH (Fast Line-of-Sight Atmospheric Analysis of Spectral Hypercubes) method [43]. After completing the atmospheric calibration, the image was stitched together using the Seamless Mosaic tool and its background value was set to 0 (ignoring background values). Cubio convolution method was selected as the sampling method for image stitching calculation to obtain satellite remote sensing images. After completing the satellite image stitching, based on the vector boundary of the study area (shp.), raster data such as the stitched satellite image, DEM elevation data, and land-use type data were used for image cropping in order to obtain the raster data of the study area extent. Subsequently, the acquired precipitation meteorological data were used to fill in the nulls using kriging interpolation to improve the accuracy of the subsequent modelling of the spatial distribution of precipitation erosivity.

2.2.3. Soil types in the Changhua River Basin

In soil science, a soil name is not only an irreplaceable and comprehensive description of the main characteristics and formation processes of a soil, but it also reflects the functions and roles of different types of soils in the ecosystem [44]. In addition, different soil categories are often closely related to soil erosion hazards because their physical and hydrological properties have important effects on the resistance to soil erosion. Therefore, this study classifies the soils in the Changhua River Basin based on the classification criteria of the World Soil Resource Reference Database (WRB), Version 4, and the specific soil categories are shown in Fig. 2, Simplified Guidelines and Codes for the World Soil Resource Reference Benchmark (WRB) Reference Soil Groups (RSGs) (IUSS WRB Working Group, 2022) [45]. As shown in Annex A - Table 1.

Among them, the Changhua River Basin contains a total of 13 soil categories, of which Acrisol (AC) and Ferralsol (FR) soils are dominant, accounting for 50.63 % and 22.35 %, respectively. Based on the diversity of the soil categories in the Changhua River Basin and their roles in soil erosion hazards, it is possible to conduct an in-depth study on the extent of the influence of different soil types on the intensity of soil erosion. From there, targeted soil protection and erosion control measures can be taken to maintain soil health and ecosystem stability.

Table 1
List of data and pre-processing methods.

Data type	Data sources	Spatial resolution	Data preprocessing
Sentinel 2 Imaging 2020–2022	Geospatial Data Cloud (http://www.gscloud.cn/)	10m	Atmospheric calibration, radiometric calibration
Landsat 8 Images 2020–2022	Geospatial Data Cloud (http://www.gscloud.cn/)	30m	Cropping and Projection Conversion
Meteorological data on precipitation	National Meteorological Science Data Center of China (http://data.cma.cn/)	30m	Kriging interpolation
DEM elevation data	Geospatial Data Cloud (http://www.gscloud.cn/)	30m	Projection conversion, splicing and cropping
Land use type data	U.S. Geological Survey (usgs, http://www.usgs.gov/)	30m	Projective transformation, visual interpretation
Reference data	Soil and Water Conservation Bulletin of Hainan Province, Hainan Provincial Statistical Yearbook	–	Data statistics

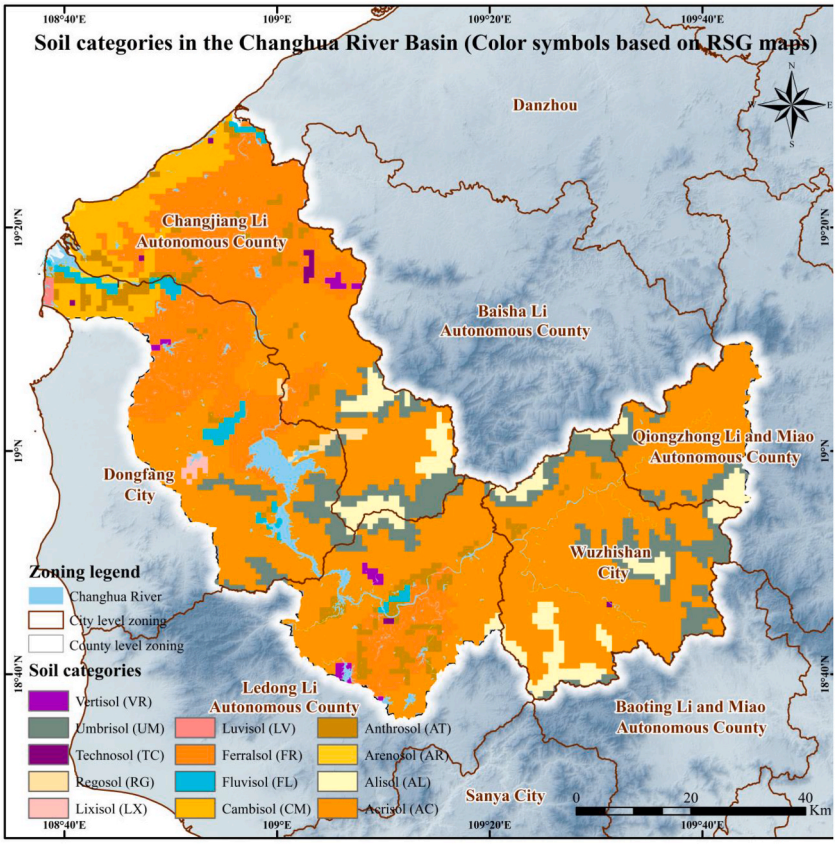

Fig. 2. Distribution of soil types in the Changhua River.

2.3. China soil loss equation (CSLE)

The China Soil Loss Equation (CSLE) was developed by Liu Baoyuan et al. [46] based on the Universal Soil Loss Equation (USLE) and the Revised Soil Loss Equation (RUSLE). The CSLE model takes into account China-specific geographic information and soil erosion characteristics, and improves the soil erosion of the Chinese national territory by combining local factors such as topography, precipitation, soil type, and vegetative cover with prediction accuracy [47–49]. Compared with the USLE and RUSLE models, the CSLE model can show higher accuracy and applicability in calculating the degree of soil erosion in China. Therefore, in this paper, the soil erosion data from 2020 to 2022 were quantified on an image-by-image, element-by-element basis, based on the CSLE model. The spatial interpolation method was used to classify the erosion intensity and to calculate the erosion modulus A. The erosion modulus A was calculated as shown in equation (1) [50] using the following equation:

$$A = R \cdot K \cdot L \cdot S \cdot B \cdot E \cdot T \tag{1}$$

where A is the soil erosion modulus in $t \cdot hm^{-2} \cdot a^{-1}$; R is the rainfall erosivity factor in $MJ \cdot mm \cdot hm^{-2} \cdot h^{-1} \cdot a^{-1}$; K is the soil erodibility factor in $t \cdot hm^2 \cdot h \cdot hm^{-2} \cdot MJ^{-1} \cdot mm^{-1}$; L is the dimensionless slope length factor; S is the dimensionless slope gradient factor; B is the dimensionless factor of vegetation cover and biological measures; E is the dimensionless factor of engineering measures; and T is the dimensionless factor of tillage measures.

2.3.1. Rainfall erosivity factor R

The rainfall erosive power is the potential ability of rainfall to cause soil erosion to occur; it depends on the amount of rainfall, rainfall intensity, precipitation duration, and other characteristics. We retrieved the daily rainfall data of the Changhua River Basin and its neighboring areas from more than eight hundred daily observations made at meteorological stations in Naikoku from 1950 to 2023. We summarized these data into monthly statistics and calculated daily rainfall data for the Changhua Creek watershed and its adjacent areas based on Equations (2)–(4) [51]:

$$\overline{R} = \sum_{k=1}^{24} \overline{R}_k \tag{2}$$

$$\overline{R}_k = \frac{1}{N}\sum_{i=1}^{N}\sum_{j=0}^{m}\left(\alpha \cdot P_{i,j,k}^{1.7625}\right) \tag{3}$$

$$\overline{WR_k} = \frac{\overline{R}_k}{\overline{R}} \tag{4}$$

where is the multi-year average annual rainfall erosivity in MJ · mm · hm^{-2} · h^{-1} · a^{-1}; k takes the values 1,2, ……, 24 (dividing the year into 24 half-months); $\overline{R}_k$ denotes the rainfall erosivity of the kth half-month in MJ · mm · hm^{-2} · h^{-1}; $P_{i,j,k}$ denotes the jth erosive rainfall of the kth half-month of year i; $\overline{WR}_k$ denotes the average rainfall erosivity of the kth half-month; and $\overline{R}_{half-moon\ k}$ denotes the proportion of the multi-year average annual rainfall erosive force $\overline{R}$. Parameter j = 0, ……, m in m refers to the number of erosive rainfall days in the kth half-month of year i (erosive rainfall days are defined as having daily rainfall greater than 10 mm); parameter i = 1, 2, ……, N (N refers to the 2020–2022 time series); and the parameter α takes the value 0.3101 in winter (January–April, October–December) and 0.3937 in summer (May–September) [52–54].

2.3.2. Slope (S) factor and slope length (L) factor

The slope length factor, also known as the topographic factor, is a numerical parameter or indicator with certain significance set to quantitatively express the morphological characteristics of landforms. It is characterized by interactions with other erosive conditions and varies under different terrain elevations, regional climates, vegetation types, and soil types [55,56]. At the same time, the combined effect of the two factors of slope length and slope gradient determines the ability of runoff to scour the soil at the surface, i.e., the rate of slope water erosion. Usually, the larger the slope, the larger the confluence; the steeper the slope, the larger the topographic drop, resulting in a higher runoff velocity and a stronger scouring ability. The slope length factor L reflects the ratio of the soil erosion levels of different slope lengths to those of the standard slope length; the steeper the slope and the longer the slope length on the cultivated land (without considering the vegetation and soil and water conservation measures), the larger the LS factor is and the stronger the soil erosion is [57,58]. Based on the digital elevation data (DEM) of the Changhua River Basin with a 30m spatial resolution, the data related to the filling depression, flow direction, flow rate, and water flow length were calculated and ultimately integrated to obtain the raster maps of the slope length factor and slope factor in the Changhua River Basin. The slope length factor is calculated as shown in equation (5) [59]:

$$L_i = \frac{\lambda_i^{m+1} - \lambda_{i-1}^{m+1}}{(\lambda_i - \lambda_{i-1}) \cdot (22.13)^m} \tag{5}$$

where λ_i and λ_{i-1} are the slope length of the ith and i-1st slope sections, respectively, and m is the slope length index, which varies with slope and takes the range of values as in Equation (6) [60]:

$$m = \begin{cases} 0.2 & \theta \le 1^\circ \\ 0.3 & 1^\circ \le \theta \le 3^\circ \\ 0.4 & 3^\circ \le \theta \le 5^\circ \\ 0.5 & \theta > 5^\circ \end{cases} \tag{6}$$

The formula for the slope coefficient is shown in Equation (7) [61]:

$$S = \begin{cases} 10.8\sin\theta + 0.03 & \theta < 5^\circ \\ 16.8\sin\theta - 0.5 & 5^\circ \le \theta \le 10^\circ \\ 21.9\sin\theta - 0.96 & \theta \ge 10^\circ \end{cases} \tag{7}$$

where S is the slope factor (dimensionless) and θ is the slope (°).

2.3.3. Soil erodibility factor (K)

The K value characterizes the difference in intrinsic soil properties, which have an important influence on the processes of water infiltration, rainfall erosion, and the runoff scouring of soil particles, which in turn affect the intensity of the erosion and its sand production. Soil erodibility is defined as the rate of soil loss due to a unit of rainfall erosive force under the standard plot conditions in the CSLE model [62]. In this study, soil erodibility factor values were calculated by combining soil data from the World Soil Database and the different soil types in the Changhua River area of Hainan Island by applying the estimation method proposed by Williams et al. [63] in the EPIC model. The formula is shown in Equation (8) [64]:

$$K = \left\{0.2 + 0.3\exp\left[-0.0256 S_{AN}\cdot\left(1 - \frac{S_{IL}}{100}\right)\right]\right\}\cdot\left(\frac{S_{IL}}{C_{LA} + S_{IL}}\right)^{0.3}\cdot \left[1.0 - \frac{0.25C}{C + \exp(3.72 - 2.95C)}\right]\cdot\left[1.0 - \frac{0.7SN_1}{SN_1 + \exp(-5.51 + 22.9SN_1)}\right] \tag{8}$$

where S_{AN} is the sand content (%), S_{IL} is the flour content (%), C_{LA} is the clay content (%), C is the organic matter content (%).

When $SN_1 = 1 - S_{AN}/100$, the K-factor value calculated according to the equation should be converted to international system

units by dividing by 7.593 [65,66], and the converted K-factor value should be assigned to different soil types in the study area to generate the soil erodibility factor raster data.

2.3.4. Soil and water conservation factor (BET)

Vegetation is the link between soil, water, and the environment in nature, and it is also one of the main factors involved in suppressing soil erosion; the level of its coverage directly affects the degree of soil erosion. Vegetation cover plays an important role in mitigating soil erosion and is an important indicator of soil erosion control, and various forms of vegetation cover can inhibit soil erosion to different degrees. To this end, we calculated the normalized vegetation index (NDVI) and the degree of vegetation cover (FVC) based on Landsat 8 imagery; finally, we completed the assignment of vegetation cover and biological measures factor B according to the land-use type. The formulae for NDVI and vegetation cover are given in Eqs. 9 and 10 [67]:

$$NDVI = \frac{N_{IR} - R}{N_{IR} + R} \tag{9}$$

where N_{IR} is the near-infrared band and R is the infrared band.

$$FVC = \frac{NDVI - NDVI_{non}}{NDVI_{veg} - NDVI_{non}} \tag{10}$$

where $NDVI_{veg}$ and $NDVI_{non}$ are fully vegetated versus bare ground or unvegetated pixel NDVI values, respectively. The values of $NDVI_{veg}$ and $NDVI_{non}$ vary over time and space due to differences in atmospheric and surface conditions, years, seasons, and regions [68,69]. Since the Changhua River Basin is located in a tropical region with abundant vegetation, the cumulative percentages of 5 % and 95 % can more accurately represent the vegetation cover in the region as confidence intervals, so we utilize the confidence intervals of 5%–95 % in order to determine the effective $NDVI_{veg}$ and $NDVI_{non}$ values of the study area, respectively. The vegetation cover of the Changhua River Basin can be obtained using the above formula, in which the value range of FVC is [0–1], and the percentage of vegetation cover ($F_{\%}$) is obtained by differentiating it by one hundred. Calculated as shown in Equation (11):

$$F_{\%} = FVC \times 100\% \tag{11}$$

After calculating the cover ($F_{\%}$), $F_{\%}$ was overlaid with the land use type data of the Changhua Creek watershed for analysis. Subsequently, the reclassification algorithm was used to complete the assignment of the bioscale factor B based on the different land use types and their overlaid vegetation cover [70]. Among them, since the water body is not affected by erosion, its assignment is 0 (The specific assignment is shown in Table 2.).

In the CSLE model, E is referred to as the factor of engineering measures, which refers to the engineering construction required to change the state of the ground surface to reduce land erosion and surface runoff, and to increase the rainfall infiltration of soil [71]. By resampling and classifying the high-resolution satellite remote sensing images of the Changhua River Basin and via manual visual interpretation, the land-use-type data of the Changhua River Basin were obtained. However, after analyzing the satellite remote sensing images and land-use-type data, no obvious scale engineering measures were found in the watershed. Referring to the study of the engineering measure factors of the neighboring Pearl River Basin conducted by Chen Yuxuan et al. [72], the engineering measure factor of the Changhua River Basin was finally determined to be 1. The specific engineering measure assignment method is shown in Table 1 in Appendix A. Since no obvious scale engineering measures were found in the watershed, the engineering measure factor for this watershed was assigned as 1.

T is the tillage factor. Tillage measures aim to maintain soil and water and suppress the amount of soil erosion. Since remote sensing images cannot accurately extract all the tillage measures, another Chinese study used an empirical formula to assign values to soil and water conservation tillage measures [73,74]. By checking the names and codes of China's crop rotation zones in "70 Years of China's Cropping System" and obtaining the cropping system zones to which the Changhua River Basin on Hainan Island belongs (Appendix-Table 1), it was determined that the Changhua River Basin on Hainan Island belongs to the Late Triple-Maturity Zone of the

Table 2
Assignment of biological measurement factors.

Land use type	Percentage covered ($F_{\%}$)	Biological Measures Factor B
Forest area	0–20 %	0.1
	20–40 %	0.08
	40–60 %	0.06
	60–80 %	0.02
	80–100 %	0.004
Grassy area	0–20 %	0.45
	20–40 %	0.24
	40–60 %	0.15
	60–80 %	0.09
	80–100 %	0.043
Cropland area	–	0.9
Construction area	–	0.23
Body of water	–	0

Low Hills Plain in South China, so the value of its tillage factor was assigned to be 0.466. A 30 m spatial resolution raster image of the T factor was generated using the re-sampling technique. The "70 Years of China's Tillage System", as shown in Table 2 in Appendix A, contains the names and codes of different crop rotation areas in China as well as the values assigned to the T-factors, and the T-factor values used in this study have been bolded.

2.4. Soil erosion intensity classification criteria

According to the Soil Erosion Classification and Grading Standard (SL190-2007), soil erosion in Hainan Province is divided into six classes. Among these classes, slight erosion is not defined as soil erosion because it is less than the permissible soil loss, so the total soil erosion area is the sum of the areas of each erosion level from mild to intense erosion. The specific erosion intensity grading criteria are shown in Table 3.

Since the Hainan area is located in the red loamy hills of southern China, the modulus of slight erosion is 0–500 $t \cdot hm^{-2} \cdot a^{-1}$, and the modulus of mild erosion is 500–2000 $t \cdot hm^{-2} \cdot a^{-1}$.

2.5. Experimental procedure

Based on the acquired remote sensing data, each erosion factor was calculated separately to construct a CSLE model for the Changhua River Basin on Hainan Island, and the grading of each intensity level and data statistics was completed according to the Classification and Grading Standard for Soil Erosion. The main characteristic factors are proposed and analyzed, and the areas potentially prone to soil erosion are inferred. To provide detailed data support and precise means of monitoring soil and water conservation work in the Changhua River Basin on Hainan Island, the specific experimental process is shown in Fig. 3.

2.6. Calculation and classification of soil erosion intensity classes

In this paper, the factors were calculated based on the CSLE model to obtain the soil erosion modulus for the Changhua River watershed in Hainan Island in 2020–2022. In this paper, different maps were generated by interpolating the R, K and B factors as covariates for cropland, woodland, grassland, shrubland and bare land using the synergistic kriging interpolation method, and setting water bodies, wetlands and impervious surfaces to 0. Subsequently, the layers of the factors were multiplied by the correlation coefficients, which is 100 in this paper to ensure that the range of magnitude of the factors is the same, through the method of map algebra, and the modulus of soil erosion in the Changhua River Basin was obtained.

2.7. Calculation of general trends in erosion in the Changhua Creek watershed

Based on the CSLE model for 2020–2022, the area and three-year rate of change (Δt_3) of each erosion intensity class were calculated separately using image-by-image statistics. The formula for calculating the rate of change is shown in Equation (12), and the statistical results are shown in Table 4.

$$\Delta t_3 = \frac{S_{2022} - S_{2020}}{S_{2020}} \tag{12}$$

where Δt_3 represents the three-year rate of change from 2020 to 2022 S_{2020}, represents the area of soil erosion at all levels in 2020, and S_{2022} represents the area of soil erosion at all levels in 2022.

2.8. CSLE model accuracy evaluation method

We first acquired high-definition satellite remote sensing images of the Changhua River basin during 2020–2022. In terms of image unit (30*30m), 300 random monitoring points were selected in the study area, which covered the main erosion intensity classes in the basin and took into account the various land use types, slopes and soil types at the same time. After obtaining the measured erosion information of the monitoring points by manual field exploration, the erosion information of each monitoring point was vectorised using GIS. And it was superimposed with the high-definition satellite remote sensing images of each year during 2020–2022 respectively, and the vectorised information of the sample points in different years was further corrected by means of manual visual

Table 3
Erosion intensity grading criteria.

Erosion intensity class	Modulus of erosion($t \cdot hm^{-2} \cdot a^{-1}$)
Micro erosion	<500
Mild erosion	500–2500
Moderate erosion	2500–5000
Intense erosion	5000–8000
Extremely strong erosion	8000–15000
Severe erosion	>15000

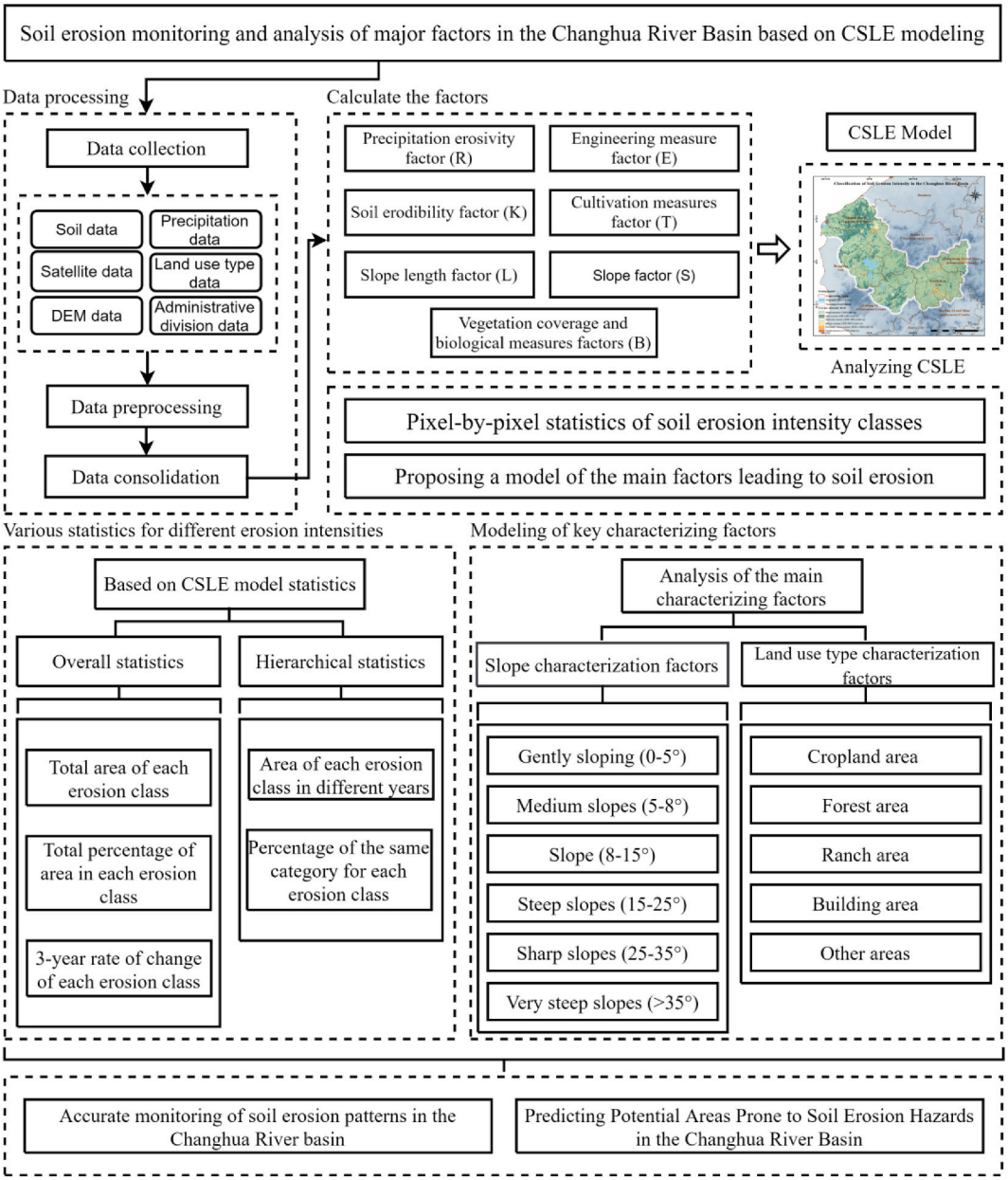

Fig. 3. Flowchart of the experiment.

Table 4
Area and trend of soil erosion in the Changhua River Basin during the period 2020–2022.

Soil erosion intensity class (t/km^2•a)	Area of and changes in soil erosion/km^2				Three-year percentage change(Δt_3)/%
	2020	2021	2022	Three-year of change	
Micro-erosion	3495.72	3596.61	4048.97	553.25	15.83 %
Mild erosion	1437.97	1366.65	991.55	−446.42	−31.05 %
Moderate erosion	214.12	202.59	149.72	−64.40	−30.08 %
Intense erosion	70.33	58.45	44.60	−25.73	−36.58 %
Extremely strong erosion	62.42	59.50	51.17	−11.25	−18.02 %
Severe erosion	39.36	36.12	33.91	−5.45	−13.85 %
Area of erosion (Mild–Severe)	1824.20	1723.31	1270.95	−553.25	−30.33 %

interpretation to obtain the validation samples. Finally, the 2020–2022 CSLE model was used as a training sample for cross-validation, and the confusion matrix was calculated to derive the overall accuracy and the Kappa coefficient, thus completing the accuracy assessment of the 2020–2022 CSLE model. Where the Kappa coefficient is calculated as shown in Equation (13).

$$K = \frac{\rho_0 - \rho_e}{1 - \rho_e} \tag{13}$$

2.9. Analysis of the main factors influencing the characterization of soil erosion

To further manage soil erosion in the Changhua Creek watershed, the key is to identify the main influencing factors and susceptible

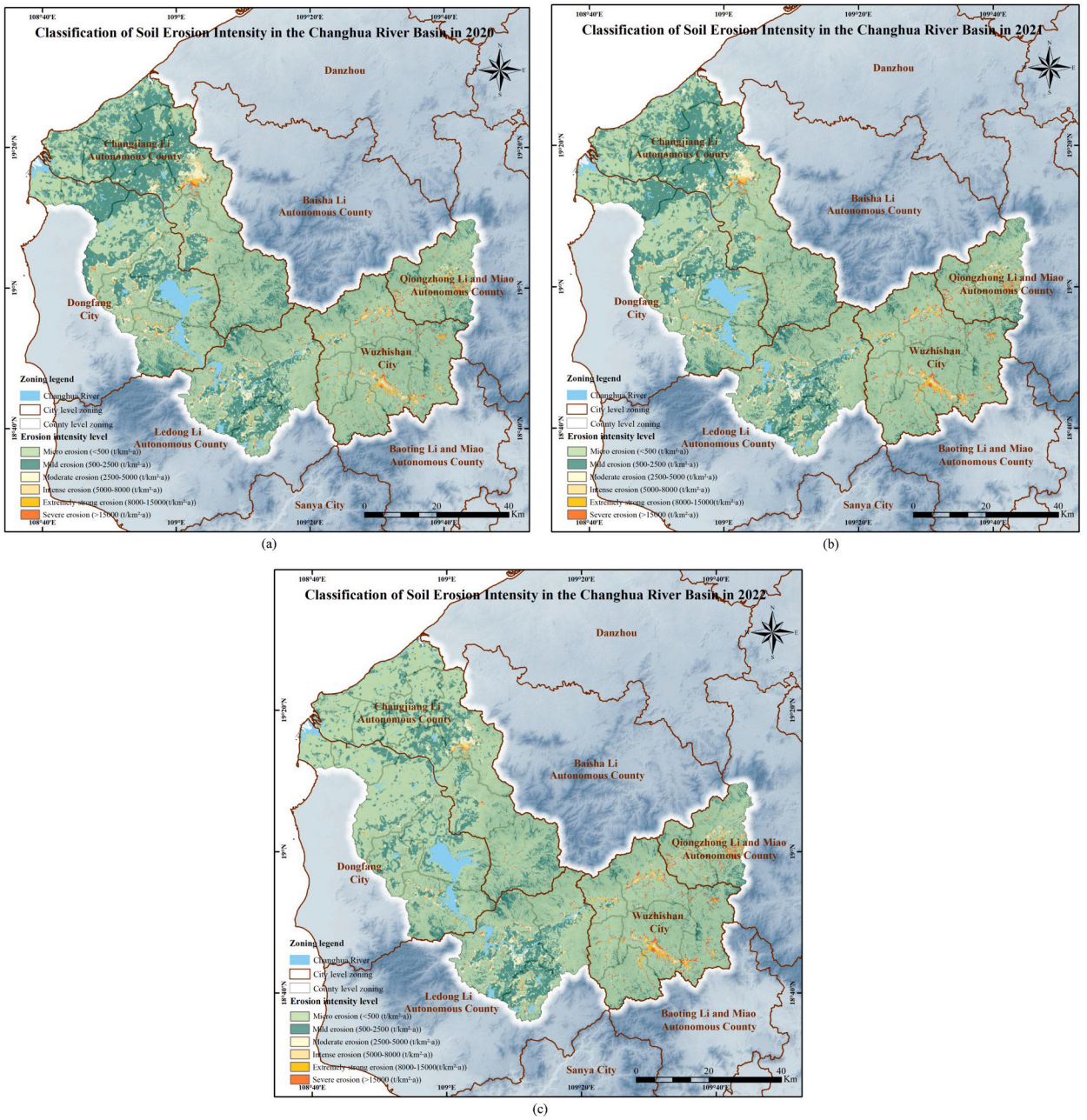

Fig. 4. Soil erosion grades in the Changhua River Basin, Hainan Province, between 2020 and 2022. (a) Grading of soil erosion intensity in the Changhua River Basin in 2020; (b) Grading of soil erosion intensity in the Changhua River Basin in 2021; (c) Grading of soil erosion intensity in the Changhua River Basin in 2022.

areas of soil erosion. According to the Chinese soil erosion equation, the grading of soil erosion intensity is mainly related to precipitation, slope, vegetation, soil, engineering measures and farming measures. The Changhua Creek watershed has a relatively uniform distribution of precipitation, has no obvious large-scale engineering measures, and belongs to the same interval of tillage measures. Therefore, we selected the land use type, slope and soil type characterization factors for analysis. In addition, since the land use type, slope characteristics and soil characteristics of the Changhua Creek watershed do not change much over time, they have better stability compared to other characterization factors, which is a significant advantage for predicting areas where disasters may occur.

2.9.1. Land-use-type characterization factors

We then further studied the relationship and influence between different land-use types and the generation and development of soil erosion in southern China, determining the main influencing factors of soil erosion and predicting the land-type areas that may be prone to disasters. To this end, we used ArcGIS 10.8 software to calculate the area and distribution of each erosion intensity level (the ratio of the area of each erosion intensity level to the total area of the land-use type) of the different land-use types of the Changhua Watershed in the period 2020–2022 and comprehensively analyze the influence of each land-use type on the occurrence and development of erosion disasters. This allowed us to provide a solid reference for the subsequent development of soil and water conservation work.

2.9.2. Slope factor

In order to further study the relationship between different slope grades and the occurrence of soil erosion, we graded the slope of the Changhua River Basin according to the ranges of 0–5°, 5–8°, 8–15°, 15–25°, 25–35°, and >35°, and six intervals, which correspond to flat and gentle slopes, medium slopes, sloping slopes, steep slopes, sharp slopes, and extremely steep slopes, respectively. The influence of slope on soil erosion was determined by analyzing the relationship between the thresholds of the different intervals and the corresponding soil erosion intensity.

2.9.3. Soil type characterization factors

Different soil types are closely related to erosion hazards. Soil types in the Changhua Creek watershed are rich and diverse, with as many as 13 surface soil types. Among them, iris loam (AC) and ferruginous loam (FR) are dominant, accounting for 50.63 % and 22.35 % of the total study area, respectively. Since different soil types have different particle sizes and structures, organic matter contents and drainage properties, they exhibit different soil retention and erosion resistance capabilities when facing erosion hazards. Therefore, the relationship between different soil types and soil erosion intensity was analyzed to determine the effect of soil type characteristics on soil erosion.

3. Results

3.1. Thematic map of spatial distribution of soil erosion intensity classes

And according to the Soil Erosion Classification and Grading Standard (SL190-2007) [75,76], each intensity of soil erosion in Hainan Province was divided into six grades, and finally the thematic map of soil erosion rate in 2020–2022 was obtained, as shown in Fig. 4. Among them, Fig. 4(a), (b) and (c) represent the grading of the degree of soil erosion in the Changhua River Basin in 2020, 2021 and 2022, respectively.

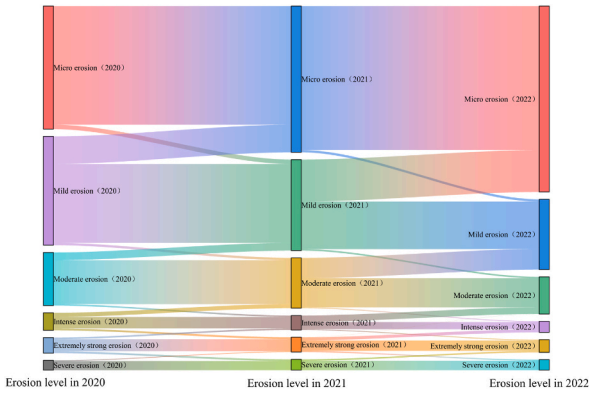

Fig. 5. Trend of soil erosion in the Changhua River Basin, 2020–2022.

3.2. Characteristics of the spatial and temporal distribution of soil erosion in the Changhua River Basin

3.2.1. Overall trend of soil erosion in the Changhua River Basin

Based on the 2020–2022 CSLE model, the area and three-year rate of change were tallied on an area-by-area basis. The area of soil erosion and the trend of change from 2020 to 2022 in the Changhua River Basin are shown in Table 4 and Fig. 5.

Fig. 4 shows that the areas of more serious soil erosion are distributed in the northeastern and southern areas of the upper reaches of the Changhua River Basin, the southwestern area of the middle reaches and the northern part of the lower reaches. Among these areas, Wuzhishan City, which is located in the southeastern part of the upper reaches of the Changhua River Basin, has the largest erosion area and the most intense degree of erosion. Table 4 and Fig. 5 indicate that, from 2020 to 2022, the total erosion area (mild to severe) of the Changhua River Basin showed a decreasing trend year by year (compared with 2020–2021, the decrease in 2021–2022 was greater), decreasing from 1824.20 km^2 to 1270.95 km^2 for a total decrease of 553.25 km^2, with a rate of change of −30.33 %. The management of mild erosion, moderate erosion, and strong erosion is particularly effective, with a rate of change of −31.05 %, −30.08 %, and −36.58 % respectively. The reductions in mild erosion and moderate erosion mainly occurred in the central and northwestern areas of the Changjiang Lizu autonomous county. The reduction in strong erosion mainly occurred in the central region of the Ledong Lizu autonomous county.

Most of these areas are located in areas of high human activity, and due to the outbreak of COVID-19 in early 2020 [77], the economic activities and productivity of the region, including aspects of land development and construction, have been severely affected [78,79]. Meanwhile, the coldness of tourism in the region, which is an important tourist area, has led to a decrease in land development and reclamation activities within the region. And the Chinese government has taken a large number of control measures to limit the scale and intensity of human activities. These measures have drastically reduced the impact of human factors on soil erosion, protected soil and water resources, promoted the recovery and growth of natural vegetation, and increased the vegetation cover in the region. At the same time, effective soil and water conservation measures were established in the region during the epidemic, improving soil quality to a certain extent and providing a positive example and reference for sustainable development. All of the above reasons contribute to a certain extent to the recovery of the soil environment in the Changhua River Basin in 2020–2022.

In addition, although very intense erosion and intense erosion throughout the entire Changhua River Basin decreased by 11.25 km^2 and 5.45 km^2 during the three years under consideration, with rates of change of −18.02 % and −13.85 %, respectively, the area of these two types of erosion intensities in Wujishan City is still increasing year by year, which is not an ideal situation. There is an urgent need to determine the causes of the higher degree of erosion in this area in order to develop corresponding protective measures.

3.2.2. Analysis of soil erosion dynamics in the Changhua River Basin

In order to further elucidate the development of soil erosion in the Changhua River Basin, we referred to statistics related to the distribution of each erosion intensity class from 2020 to 2022 and undertook the dynamic monitoring of each erosion class's proportion and change trend year by year. This provided technical and data support for the next step of soil and water conservation work. The specific analysis results are shown in Table 5 and Fig. 6.

The soil erosion areas of each grade in Hainan Province during the period 2020–2022 were summarized, and the percentage of each erosion intensity in each year and the rate of change of the area percentage over the three years were calculated. Table 5 and Fig. 6 show that, during the period from 2020 to 2021, the total erosion area only decreased by 1.90 %, with the decrease in the area of mild erosion dominated by a total decrease of 1.34 %. Although the other erosion intensity percentages exhibit a decreasing trend, the fluctuations are less than 0.3 %, and the changes are small. Moreover, in 2021–2022, the total erosion area was reduced by 26.25 %; mild erosion and moderate erosion were reduced by 7.05 % and 1.00 %, respectively, and the effectiveness of soil erosion control was remarkable. Although the proportion of strong erosion and very strong erosion also decreased to a certain extent, severe erosion was only reduced by 0.04 %, and it is therefore necessary to focus on the areas of severe erosion in future soil and water conservation work. Over these three years, the area and percentage of slight erosion continued to increase, from 3495.72 km^2 in 2020 to 4048.97 km^2 in 2022, with the percentage increasing from 65.71 % to 76.11 %. The area and percentage of mild erosion, moderate erosion, intense erosion, and very intense erosion all showed a decreasing trend, and the total erosion percentage decreased by 10.40 %. Since the degree of slight erosion is lower than the permissible soil loss, it is not defined as soil erosion. Therefore, in general, soil erosion in the Changhua River Basin has effectively been improved.

Table 5
Area share of each soil erosion class in the Changhua River Basin, 2020–2022.

Soil erosion intensity class ($t/km^2 \bullet a$)	Area of and changes in soil erosion/km^2						
	2020	Percentage of each grade	2021	Percentage of each grade	2022	Percentage of each grade	Three-year percentage change(Δt_3)/%
Micro-erosion	3495.72	65.71 %	3596.61	67.61 %	4048.97	76.11 %	10.40 %
Mild erosion	1437.97	27.03 %	1366.65	25.69 %	991.55	18.64 %	−8.39 %
Moderate erosion	214.12	4.03 %	202.59	3.81 %	149.72	2.81 %	−1.22 %
Intense erosion	70.33	1.32 %	58.45	1.09 %	44.6	0.84 %	−0.48 %
Extremely strong erosion	62.42	1.17 %	59.5	1.12 %	51.17	0.96 %	−0.21 %
Severe erosion	39.36	0.74 %	36.12	0.68 %	33.91	0.64 %	−0.10 %
Area of erosion (Mild–Severe)	1824.20	34.29 %	1723.31	32.39 %	1270.95	23.89 %	−10.40 %

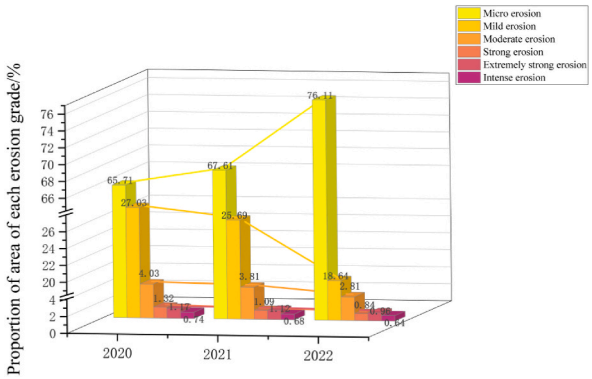

Fig. 6. Trend of the area share of each soil erosion class in the Changhua River Basin, 2020–2022.

3.3. CSLE model accuracy evaluation

Accuracy assessment of the 2020–2022 CSLE model was completed based on the confusion matrix, overall accuracy, and Kappa coefficient. The overall accuracy and kappa coefficients are shown in Table 6, and some of the monitoring points are shown in Appendix A. Fig. 1.

3.4. Statistics and analysis of erosion area by characterization factor

In this paper, after analyzing and deriving the main characteristic factors leading to the erosion disaster in Changhua Creek watershed, we superimposed the calculation of each erosion intensity level and each characteristic factor in Changhua Creek watershed from 2020 to 2022, statistically calculated the distribution data of each erosion intensity level in the different characteristic factor intervals, determined the impact of the critical value of characteristic factor in different intervals on erosion, and revealed the impact of each characteristic factor on erosion.

3.4.1. Erosion results and trend analysis across intervals in the land use type characterization

The results of the overlay analysis of the land use type characterization factors with the erosion classes are shown in Tables 7 and 8 and in Fig. 7.

Tables 7 and 8 and Figs. 7 and 8 show that, among all of the land-use types with different erosion levels, forest land accounted for 85.69 %, 84.66 %, and 82.74 % of the total areas of micro-erosion in 2020–2022. These values, which are all greater than 80 %, indicate that the micro-erosion was mainly concentrated in forest land, which further demonstrates that forest land is able to optimize the soil's physicochemical properties, improve the soil vigor, and provide strong soil and water conservation abilities. The total area of forest land in the Changhua River Basin is about 3423.17 km^2, accounting for about 64.35 % of the area of the basin, which greatly reduces the occurrence of erosion disasters and, to a certain extent, shows the importance of forest areas for soil and water conservation.

The mild, moderate, and intense erosion in the Changhua River Basin mainly occurs in cultivated areas, and, in 2020, the areas of mild, moderate, and intense erosion in cultivated areas measured 874.88 km^2, 74.82 km^2, and 17.49 km^2, respectively, accounting for 60.84 %, 34.94 %, and 24.87 % of the respective erosion types. Meanwhile, the percentages of the same erosion types for the very intense and intense erosion grades in the cultivated areas were less than 5 %. This indicates that arable land, a non-natural land-use type, is influenced by human activities, such as monocultures or chemical pesticide spraying. This leads to the occurrence of mild soil erosion to a certain extent, but it still has a weak soil and water conservation capacity, so that these regions do not experience more serious soil erosion. In addition, the occurrence of overall soil erosion in pasture is more dispersed, mostly manifesting as moderate, strong, and very strong erosion, and the same type accounts for a small percentage. Over the three studied years, the overall trend of the erosion situation gradually improved, but the high erosion levels (strong–intense) are still serious; the average percentage across the three years is 53.58 %, so pasture areas require more intensive management of high erosion levels.

Table 7 shows that very strong erosion and intense erosion mainly occurred in construction land. The area of built land in the Changhua River Basin is about 260 km^2, while the area of built land with intense erosion in 2020, 2021, and 2022 reached values of

Table 6
CSLE model accuracy evaluation 2020–2022.

CSLE Model	Overall Accuracy	Kappa
2020	91.55 %	0.8299
2021	95.31 %	0.9036
2022	88.47 %	0.7375

Table 7
Area statistics for each erosion intensity class in the land-use-type characterization factor in the Changhua River Basin, 2020–2022.

Year	Type of soil utilization	Area statistics by erosion intensity class/km^2						Total erosion area/km^2
		Micro-erosion	Mild erosion	Moderate erosion	Intense erosion	Extremely strong erosion	Severe erosion	
2020	Cultivated area	266.2	**874.88**	**74.82**	**17.49**	2.78	0.2	1236.37
	Forest area	**2995.43**	397.89	24.25	3.03	1.43	1.14	3423.17
	Ranch area	94.62	147.54	33.75	13.55	11.2	4.72	305.38
	Construction area	66.51	3.55	80.66	36	**46.77**	**32.95**	266.44
	Other usage areas	72.96	14.11	0.64	0.26	0.24	0.35	88.56
	Total area	3495.72	1437.97	214.12	70.33	62.42	39.36	5319.92
2021	Cultivated area	300.9	**799.6**	**69.35**	**14.33**	1.7	0.2	1186.08
	Forest area	**3045.03**	399.03	24.48	2.39	1.17	1.3	3473.4
	Ranch area	60.64	142.32	32.06	13.31	11.31	4.25	263.89
	Construction area	76.13	11.45	76.14	28.17	**45.09**	**30.06**	267.04
	Other usage areas	113.91	14.25	0.56	0.25	0.23	0.31	129.51
	Total area	3596.61	1366.65	202.59	58.45	59.5	36.12	5319.92
2022	Cultivated area	425.38	**534.63**	**49.55**	**7.51**	0.73	0.18	1017.98
	Forest area	**3349.92**	363.01	20.67	1.58	0.96	1.28	3737.42
	Ranch area	84.32	72.2	27.7	11.9	9.44	4.36	209.92
	Construction area	106.1	9.55	51.37	23.43	**39.75**	**27.85**	258.05
	Other usage areas	83.25	12.16	0.43	0.18	0.29	0.24	96.55
	Total area	4048.97	991.55	149.72	44.6	51.17	33.91	5319.92

Table 8
Share of the same type in each erosion class in the land-use-type characterization factors in the Changhua River Basin, 2020–2022.

Year	Type of soil utilization	Percentage of the same type for each soil erosion class						Percentage of total eroded area
		Micro-erosion	Mild erosion	Moderate erosion	Intense erosion	Extremely strong erosion	Severe erosion	
2020	Cultivated area	7.62 %	**60.84 %**	**34.94 %**	**24.87 %**	4.45 %	0.51 %	23.24 %
	Forest area	**85.69 %**	27.67 %	11.33 %	4.31 %	2.29 %	2.90 %	64.35 %
	Ranch area	2.71 %	10.26 %	15.76 %	19.27 %	17.94 %	11.99 %	5.74 %
	Construction area	1.90 %	0.25 %	37.67 %	51.19 %	**74.93 %**	**83.71 %**	5.01 %
	Other usage areas	2.09 %	0.98 %	0.30 %	0.37 %	0.38 %	0.89 %	1.66 %
2021	Cultivated areas	8.37 %	**58.51 %**	**34.23 %**	**24.52 %**	2.86 %	0.55 %	22.30 %
	Forest area	**84.66 %**	29.20 %	12.08 %	4.09 %	1.97 %	3.60 %	65.29 %
	Ranch area	1.69 %	10.41 %	15.83 %	22.77 %	19.01 %	11.77 %	4.96 %
	Construction area	2.12 %	0.84 %	37.58 %	48.20 %	**75.78 %**	**83.22 %**	5.02 %
	Other usage areas	3.17 %	1.04 %	0.28 %	0.43 %	0.39 %	0.86 %	2.43 %
2022	Cultivated areas	10.51 %	**53.92 %**	**33.10 %**	**16.84 %**	1.43 %	0.53 %	19.14 %
	Forest area	**82.74 %**	36.61 %	13.81 %	3.54 %	1.88 %	3.77 %	70.25 %
	Ranch area	2.08 %	7.28 %	18.50 %	26.68 %	18.45 %	12.86 %	3.95 %
	Construction area	2.62 %	0.96 %	34.31 %	52.53 %	**77.68 %**	**82.13 %**	4.85 %
	Other usage areas	2.06 %	1.23 %	0.29 %	0.40 %	0.57 %	0.71 %	1.81 %

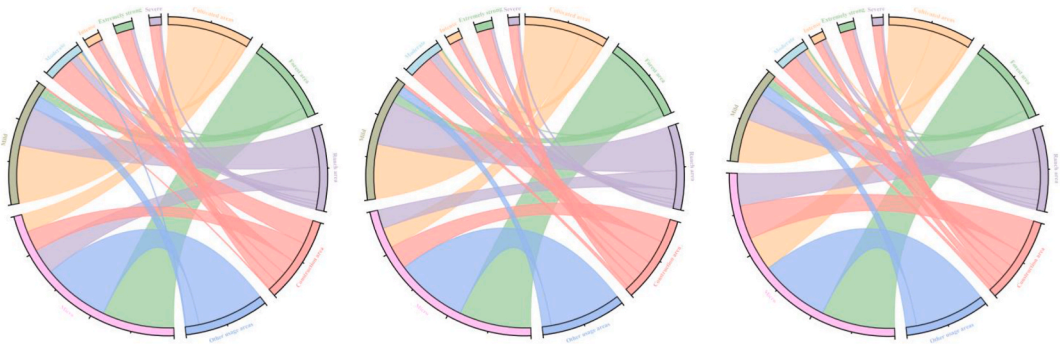

Figure 7. 2020–2022 trends in erosion intensity classes by land-use type.

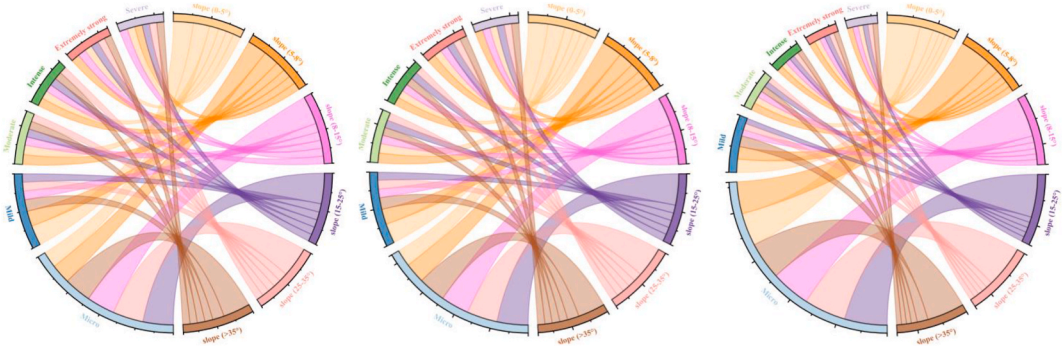

Fig. 8. Trends in each erosion intensity class for different slope intervals, 2020–2022.

32.95 km^2, 30.06 km^2, and 27.85 km^2, respectively, accounting for 83.71 %, 83.22 %, and 82.13 % of the area of intense erosion in that year. The area of intense erosion across the three years exhibits a decreasing trend, but it remains at a high level. This indicates that construction sites are susceptible to high-grade soil erosion. It is therefore necessary to pay attention to these areas when carrying out soil and water conservation work, increasing management efforts and improving management strategies based on this area's unique geographic characteristics.

3.4.2. Erosion results and trend analysis of intervals in slope characterization

The effects of different slope intervals on soil erosion hazard can be obtained by superimposing six intervals of slope 0–5°, 5–8°, 8–15°, 15–25°, 25–35°, and >35° with the erosion intensity class. Tables 9 and 10 and Fig. 8 show the relationship between slope and the distribution of erosion intensity classes for the years 2020–2022.

Tables 9 and 10 and Fig. 8 show that the total area of erosion under the different slope classes is ranked as follows: flat and gentle slope > steep slopes > sloping slopes > sharp slopes > medium slopes > extremely steep slopes. Regarding the overall trend, the erosion area of each intensity class decreased year by year. In the areas with a slope of 0–5°, the erosion types are mainly slight erosion and mild erosion, followed by moderate erosion, with the three-year average proportions of 25.92 %, 55.34 %, and 50.70 %, respectively. The areas of mild and moderate erosion gradually decreased over the three-year period, from 862.01 km^2 to 116.06 km^2

Table 9
Area statistics for each erosion intensity class in the slope characterization factor for the Changhua River Basin, 2020–2022.

Year	Slope/°	Area statistics by erosion intensity class/km^2						Total erosion area/km^2
		Micro-erosion	Mild erosion	Moderate erosion	Intense erosion	Extremely strong erosion	Severe erosion	
2020	0–5 (flat and gentle slope)	859.84	**862.01**	**116.06**	**32.55**	**24.91**	**10.07**	1905.44
	5–8 (medium slope)	298.22	178.06	38.38	14.88	14.45	7.92	551.91
	8–15 (sloping slope)	744.41	135.57	32.77	13.94	15.23	**14.35**	956.29
	15–25 (steep slope)	982.82	146	17.68	6.39	6.35	5.65	1164.89
	25–35 (sharp slope)	494.62	82.58	5.74	1.63	1.12	1.11	586.79
	>35 (extremely steep slope)	115.82	33.75	3.48	0.94	0.37	0.26	154.61
	Total area	3495.72	1437.97	214.12	70.33	62.42	39.36	5319.92
2021	0–5 (flat and gentle slope)	848.38	**791.79**	**106**	**25.4**	**24.61**	**9.01**	1805.19
	5–8 (medium slope)	307.82	174.64	36.49	12.16	13.87	7.77	552.76
	8–15 (sloping slope)	744.47	136.84	32.76	12.24	13.88	**13.03**	953.22
	15–25 (steep slope)	1085.7	146.68	18.07	6.26	5.74	5.01	1267.47
	25–35 (sharp slope)	494.33	82.76	5.89	1.57	1.12	1.08	586.75
	>35 (extremely steep slope)	115.9	33.93	3.38	0.82	0.28	0.22	154.54
	Total area	3596.61	1366.65	202.59	58.45	59.5	36.12	5319.92
2022	0–5 (flat and gentle slope)	1197.73	**477.12**	**68.22**	**20.36**	**18.93**	**8.13**	1790.49
	5–8 (medium slope)	363.61	141.35	27.46	9.11	11.76	7.41	560.7
	8–15 (sloping slope)	762.47	127.52	28.13	8.33	12.69	**12.47**	951.61
	15–25 (steep slope)	1106.8	135.3	17.68	4.89	6.35	4.85	1275.87
	25–35 (sharp slope)	501.04	76.94	5.33	1.34	1.14	0.95	586.74
	>35 (extremely steep slope)	117.33	33.33	2.9	0.56	0.3	0.1	154.52
	Total area	4048.97	991.55	149.72	44.6	51.17	33.91	5319.92

in 2020 to 477.12 km^2 and 68.22 km^2 in 2022, with a change rate of −44.7 % and −41.2 %, respectively. Since this area accounts for a large proportion of the total area of the Changhua River Basin, and the three-year average proportion of strong and very strong erosion in this area is 45.13 % and 39.42 %, respectively, it indicates that this area is a key area prone to strong and very strong erosion.

In the areas with 5–8° slopes, the area of land with slight erosion are increasing year by year, and the area of both mild and intense erosion classes is decreasing year by year. The slightly eroded area increased from 298.22 km^2 in 2020 to 363.61 km^2 in 2022, with the proportion rising from 8.53 % to 18.83 %, and the overall trend of soil and water conservation gradually improved.

The areas with 8–15° slopes are smaller for all types of erosion due to the smaller overall land area, but this area is more prone to violent erosion and has the highest percentage of violent erosion, with a three-year average of up to 36.43 %. Moreover, there is no significant downward trend, so there is an urgent need to focus on the management of these area.

Finally, in order to determine the characteristics of the main influencing factors that lead to the occurrence of soil erosion, the land-use-type characterization factors were superimposed onto the slope characterization factors. It was found that areas with slopes greater than 15° have a greater range of overlap with forested areas, making it possible to maintain a low erosion rate in steep areas that are highly susceptible to soil erosion. This indicates that land-use-type characteristics rather than slope characteristics are the main factor contributing to soil erosion in this area, suggesting that forested areas are more effective at inhibiting soil erosion.

3.4.3. Erosion results and trend analysis of intervals in soil type characterization

In this study, the average erosion intensity rating for 2020–2022 was superimposed on the 13 major soil types. It is possible to reveal differences in the performance of different soil types in the face of erosion and thus assess their relative strength against erosion. The results are summarized in Table 11.

By analysing Tables 11 and it can be seen that the Technosol (TC) soil type has only 5.88 % of its total area of slight erosion, moderate erosion and intense up to 52.94 % and 11.76 %, which is the largest percentage of the same erosion class; Ferralsol (FR) and Fluvisol (FL) soil types both have more than 40 % of mild erosion; furthermore, the Very strong erosion is relatively more likely to occur in the Lixisol (LX) soil type, which accounts for 6.25 % of the total area of the type, while all other soil types have less than 3 % of their own total area; severe erosion is relatively more likely to occur in the Acrisol (AC) soil type, which accounts for 1.27 % of its total area, while all other soil types have less than 0.4 %. The above data show that Technosol, Ferralsol and Fluvisol soil types are generally less resistant to erosion hazards, with the non-erosion area (minor erosion) being less than 55 per cent of the total area, while the high level erosion hazards (very strong erosion and severe erosion hazards) are relatively more likely to occur in the Lixisol and Acrisol soil types. Therefore, there is an urgent need to take effective measures to enhance the erosion resistance of these soil types, especially the prevention and management of high-level erosion hazards.

Table 10
Homogeneous share of each erosion class in the slope characterization factors in the Changhua River Basin, 2020–2022.

Year	Slope/°	Percentage of the same type for each soil erosion class						Area proportion
		Micro-erosion	Mild erosion	Moderate erosion	Intense erosion	Extremely strong erosion	Severe erosion	
2020	0–5 (flat and gentle slope)	24.60 %	**59.95 %**	**54.20 %**	**46.28 %**	**39.91 %**	**25.58 %**	35.82 %
	5–8 (medium slope)	8.53 %	12.38 %	17.92 %	21.16 %	23.15 %	20.12 %	10.37 %
	8–15 (sloping slope)	21.29 %	9.43 %	15.30 %	19.82 %	24.40 %	**36.46 %**	17.98 %
	15–25 (steep slope)	28.11 %	10.15 %	8.26 %	9.09 %	10.17 %	14.35 %	21.90 %
	25–35 (sharp slope)	14.15 %	5.74 %	2.68 %	2.32 %	1.79 %	2.82 %	11.03 %
	>35 (extremely steep slope)	3.31 %	2.35 %	1.63 %	1.34 %	0.59 %	0.66 %	2.91 %
2021	0–5 (flat and gentle slope)	23.59 %	**57.94 %**	**52.32 %**	**43.46 %**	**41.36 %**	**24.94 %**	33.93 %
	5–8 (medium slope)	8.56 %	12.78 %	18.01 %	20.80 %	23.31 %	21.51 %	10.39 %
	8–15 (sloping slope)	20.70 %	10.01 %	16.17 %	20.94 %	23.33 %	**36.07 %**	17.92 %
	15–25 (steep slope)	30.19 %	10.73 %	8.92 %	10.71 %	9.65 %	13.87 %	23.82 %
	25–35 (sharp slope)	13.74 %	6.06 %	2.91 %	2.69 %	1.88 %	2.99 %	11.03 %
	>35 (extremely steep slope)	3.22 %	2.48 %	1.67 %	1.40 %	0.47 %	0.61 %	2.90 %
2022	0–5 (flat and gentle slope)	29.58 %	**48.12 %**	**45.57 %**	**45.65 %**	**36.99 %**	**23.98 %**	33.66 %
	5–8 (medium slope)	8.98 %	14.26 %	18.34 %	20.43 %	22.98 %	21.85 %	10.54 %
	8–15 (sloping slope)	18.83 %	12.86 %	18.79 %	18.68 %	24.80 %	**36.77 %**	17.89 %
	15–25 (steep slope)	27.34 %	13.65 %	11.81 %	10.96 %	12.41 %	14.30 %	23.98 %
	25–35 (sharp slope)	12.37 %	7.76 %	3.56 %	3.00 %	2.23 %	2.80 %	11.03 %
	>35 (extremely steep slope)	2.90 %	3.36 %	1.94 %	1.26 %	0.59 %	0.29 %	2.90 %

Table 11
Area statistics and percentage of each erosion intensity class in the 2020–2022 Changhua Creek watershed soil type characterization factor.

Year	Soil Type	Area statistics by erosion intensity class/km^2						Total erosion area/ km^2
		Micro-erosion	Mild erosion	Moderate erosion	Intense erosion	Extremely strong erosion	Severe erosion	Percentage of eroded area
2020–2022	Vertisol (VR)	15.33	8.88	1.61	1.61	0.81	0.00	28.25
		54.29 %	31.43 %	5.71 %	5.71 %	2.86 %	0.00 %	0.54 %
	Umbrisol	374.45	87.96	9.68	1.61	0.81	0.81	475.33
	(UM)	78.78 %	18.51 %	2.04 %	0.34 %	0.17 %	0.17 %	9.03 %
	Technosol	**0.81**	4.04	**7.26**	**1.61**	0.00	0.00	13.72
	(TC)	**5.88 %**	29.41 %	**52.94 %**	**11.76 %**	0.00 %	0.00 %	0.26 %
	Regosol (RG)	18.56	3.23	0.00	0.81	0.00	0.00	22.60
		82.14 %	14.29 %	0.00 %	3.57 %	0.00 %	0.00 %	0.43 %
	Lixisol (LX)	5.65	4.04	1.61	0.81	**0.81**	0.00	12.91
		43.75 %	31.25 %	12.50 %	6.25 %	**6.25 %**	0.00 %	0.25 %
	Luvisol (LV)	4.04	0.00	0.00	0.00	0.00	0.00	4.04
		100.00 %	0.00 %	0.00 %	0.00 %	0.00 %	0.00 %	0.08 %
	Ferralsol (FR)	543.12	**551.19**	65.37	8.88	4.84	2.42	1175.82
		46.19 %	**46.88 %**	5.56 %	0.75 %	0.41 %	0.21 %	**22.35 %**
	Fluvisol (FL)	37.12	**30.67**	2.42	0.81	0.00	0.00	71.02
		52.27 %	**43.18 %**	3.41 %	1.14 %	0.00 %	0.00 %	1.35 %
	Cambisol	202.56	67.79	2.42	0.00	0.00	0.00	272.77
	(CM)	74.26 %	24.85 %	0.89 %	0.00 %	0.00 %	0.00 %	5.18 %
	Anthrosol	121.86	85.54	5.65	3.23	2.42	0.81	219.51
	(AT)	55.51 %	38.97 %	2.57 %	1.47 %	1.10 %	0.37 %	4.17 %
	Arenosol	13.72	4.04	1.61	0.00	0.00	0.00	19.37
	(AR)	70.83 %	20.83 %	8.33 %	0.00 %	0.00 %	0.00 %	0.37 %
	Alisol (AL)	214.66	61.33	4.84	1.61	0.00	0.00	282.45
		76.00 %	21.71 %	1.71 %	0.57 %	0.00 %	0.00 %	5.37 %
	Acrisol (AC)	2040.93	400.28	98.46	33.09	57.30	**33.89**	2663.94
		76.61 %	15.03 %	3.70 %	1.24 %	2.15 %	**1.27 %**	**50.63 %**

4. Discussion

4.1. Applicability advantages of the CSLE model

The China Soil Loss Equation (CSLE) is a computational soil erosion model based on soil erosion characteristics and data gathered in China. The model integrates factors such as topography, land use, rainfall, and the soil erosion rate, and has strong scientific validity and accuracy, so it is widely used in the quantitative evaluation of soil erosion in China. Moreover, the CSLE model can exhibit higher accuracy when grading the soil erosion intensity in the Changhua River Basin. This is because the CSLE model is based on a large amount of local data and research results, which more accurately reflect the actual situation of local soil erosion; this means that the model exhibits advantages in terms of data adaptability. In addition, compared with the RUSLE and USLE models, the angular range of the LS factor equation in the CSLE was changed from 10° to 14°. Moreover, based on the empirical formulas of engineering measures and different crop rotation areas in China, the E-factor of engineering measures and the T-factor of tillage measures were proposed, and the related assignment methods were developed. At the same time, the land-use type and vegetation cover were superimposed and analyzed, and the assignment of factor B was completed via reclassification, which can effectively increase the weight of the vegetation and land-use-type factors in China's soil erosion equation. Therefore, the Chinese CSLE model is more clearly aligned with Chinese environmental characteristics than the USLE and RUSLE models, and it is also more suitable for the Changhua River Basin, which has complex topography.

4.2. Overall trends in soil erosion intensity, 2020–2022

Although the Changhua River Basin is dominated by slight erosion, the total soil erosion area is the sum of the total area with mild or higher levels of erosion; this is because slight erosion leads to levels of erosion that are lower than the permissible soil loss, so it is not defined as soil erosion. Thus, it is clear from the analysis that the soil environment in the Changhua River Basin is relatively fragile, and there is an urgent need to prevent and control soil erosion. In 2020, after a comprehensive soil and water conservation project was carried out by the Hainan Water Affairs Department [80], the soil environment was further improved, and the total area of erosion was reduced from 1824.20 km^2 to 1270.95 km^2, with the total area share decreasing by 10.40 %. The area of each erosion class was also reduced to different degrees. Specifically, the area share of mild erosion decreased the most, reaching 8.39 %, while the area share of strong-to-severe erosion decreased by less than 1 %. Therefore, future soil and water conservation efforts need to focus on areas with high erosion levels.

4.3. Influence of land use type characterization factors on soil erosion intensity

The factors characterizing land-use types are closely related to several factors in the CSLE model. Different land-use types exhibit significant differences in soil and water conservation, vegetation cover, and soil texture, and these factors affect the surface runoff and soil erosion processes to different degrees. The main land-use types in the Changhua River Basin are cropland, forest land, building land, and pasture land. In 2022, for example, 82.74 % of the non-erosion areas were in forested areas, so it is known that forests have better soil and water conservation capacity, which can effectively reduce the occurrence of soil erosion; mild, moderate, and strong erosion occurs more often in cropland areas, and the proportions of the same types are 53.92 %, 33.10 %, and 16.84 %, respectively. This is due to the use of monocultures and the serious misuse of pesticides, which cause the more serious erosion problems to occur in cultivated land. In order to solve the soil erosion problem in this region, it is necessary to formulate scientific measures to return farmland to forests; while high-grade erosion mostly occurs in construction land, the proportion of the same type of land with very strong and severe erosion in this region is as high as 77.68 % and 82.13 %, respectively, so there is an urgent need to strengthen the land planning and management in this region, limit the scale of development, reduce the overuse of the land, and promote the restoration of the ecological environment.

4.4. Influence of slope-type characterization factors on soil erosion intensity

Slope is an important indicator of topographic factors; the steeper the slope, the higher the risk of soil erosion. Erosion varies across different slope types. Therefore, slopes are graded according to six intervals: 0–5°, 5–8°, 8–15°, 15–25°, 25–35°, and >35°, corresponding to gentle slopes, moderate slopes, slopes, steep slopes, sharp slopes, and very steep slopes, respectively. The total erosion area was ranked as follows: flat and gentle slopes > steep slopes > slopes > sharp slopes > medium slopes > extremely steep slopes. Erosion hazards mainly occurred in areas with gentle slopes of 0–5°, with an average proportion of 35.37 %. This is because many people gather in these areas, the influence of human factors is sizeable, and irrational land use and excessive development and utilization lead to the occurrence of erosion disasters on a large scale. Compared with other slope intervals, the 8–15° slope area is more prone to intense erosion, and the decline over the three studied years was only 0.31 %. This means that this kind of area is relatively difficult to manage, and scientific and reasonable ecological restoration measures should be further developed for these areas. Although the risk of soil erosion is higher as the slope increases, the erosion hazard is not serious in areas with slopes greater than 15°. This is because the region is mostly forested, and forested land plays a key role in suppressing soil erosion.

4.5. Influence of soil type characterization factors on soil erosion intensity

Different types of soil have different abilities to resist soil erosion due to differences in their particle size, structure, organic matter content and drainage properties. Therefore, soil types are closely related to soil erosion hazards. In this paper, by superimposing the 3-year average erosion class intensity changes in the Changhua River Basin with the 13 major soil categories in the basin, the characteristics of Acrisol soil type significantly affected the development of soil erosion disasters in the area because it dominated the basin, and the soil erosion disaster resistance capacities of Technosol, Ferralsol, and Fluvisol categories were generally poor, is the high incidence of soil erosion disasters. Corresponding measures should be formulated according to the physical and chemical properties of different soil types to reduce the occurrence of soil erosion disasters in the Changhua River Basin.

5. Conclusions

This study utilized GIS and RS technologies in combination with the soil erosion model of the Changhua River Basin in China, aiming to accurately monitor the trend and spatial distribution of soil erosion intensity in the Changhua River Basin during the period of 2020–2022. The experimental results showed that in the spatial dimension, the areas with more serious soil erosion were mainly distributed in the northeastern and southern areas of the upper reaches of the Changhua River Basin, the southwestern area of the middle reaches, and the northern area of the lower reaches. Among them, Wuzhishan City, located in the southeastern part of the upper reaches of the Changhua River Basin, has the largest erosion area and the most serious degree of erosion. In the time dimension, the total area of erosion in the Changhua River Basin shows a decreasing trend year by year, with a more pronounced decrease from 2021 to 2022 than from 2020 to 2021. The total soil erosion area decreased from 1824.20 km^2 to 1270.95 km^2, the total area decreased by 553.25 km^2, and the rate of change was −30.33 %. Among them, the effect of mild, moderate and severe soil erosion treatment is especially remarkable, with the percentage of area decreased by 31.05 %, 30.08 % and 36.58 % respectively.

In order to further study the main factors of soil erosion, the in-depth study of CSLE model and its construction principle in this paper puts forward the characteristics of land use type, slope characteristics and soil type characteristics. By further analyzing the relationship between the critical values of different intervals of these three characteristics and the generation and development of soil erosion, the influence mechanism of each characteristic on soil erosion can be better understood. In particular, mild erosion is mainly concentrated in forested areas and Technosol, Ferralsol and Fluvisol soil type zones. Moderate and severe erosion occurs in cropland and areas with slopes between 0 and 5°. Intense erosion is concentrated in built-up areas, areas with slopes between 8° and 15°, and areas with the soil types Lixisol and Acrisol. At slopes greater than 15°, slope is no longer a major factor in erosion, and the presence of woodland greatly reduces erosion. To summarize, in areas with slopes of 0–5°, the policy of returning farmland to forests and grazing land to grassland should be adopted in order to further enhance the soil's ability to conserve water and soil, and to improve the erosion resistance of the three types of soils, Technosol, Ferralsol and Fluvisol. At the same time, special attention should be paid to

construction areas and areas with slopes of 8°–15°, and scientific soil and water conservation measures and ecological restoration measures should be taken to reduce the intensity of soil and water erosion and comprehensively protect the ecological environment of Changhua Creek watershed.

Data availability statement

The availability of these data is restricted. The data were obtained from third parties from whom the authors have obtained permission to access them. As the data related to the research in this paper are confidential, they are not stored in a public repository. All data relevant to this research can be obtained from the authors with permission from the third party.

Funding

This research was funded by the Geological survey project of China Geological Survey(No.DD20220956); the Major Project of High-Resolution Earth Observation System of China (No. GFZX0404130304); the Open Fund of Hunan Provincial Key Laboratory of Geo-Information Engineering in Surveying, Mapping and Remote Sensing, Hunan University of Science and Technology (No. E22201); a grant from State Key Laboratory of Resources and Environmental Information System(NO); and the Innovation Capability Improvement Project of Scientific and Technological Small and Medium-sized Enterprises in Shandong Province of China (No. 2021TSGC1056).

CRediT authorship contribution statement

Xiwen Li: Supervision, Methodology, Funding acquisition. **Zhenqi Song:** Writing – original draft, Methodology, Data curation, Conceptualization. **Yuefeng Lu:** Writing – review & editing, Supervision, Methodology, Formal analysis, Conceptualization. **Baofeng Weng:** Software, Resources, Investigation. **Jing Li:** Project administration, Methodology. **Yanru Liu:** Project administration, Methodology. **Zhenli Wang:** Software, Resources. **You Gou:** Funding acquisition, Formal analysis.

Declaration of competing interest

The authors declare that they have no known competing financial interests or personal relationships that could have appeared to influence the work reported in this paper.

Acknowledgements

Ensure that all individuals included in this section agree to the acknowledgements. The authors would also like to thank the provider of the administrative district data used in this paper; the Resource and Environmental Science Data Center of the Chinese Academy of Sciences (https://www.resdc.cn/, accessed February 12, 2024). In addition, the authors would like to thank the provider of high resolution satellite imagery of the Changhua River Basin; Geospatial Data Cloud (https://www.gscloud.cn/, accessed March 10, 2024).

Appendix A

Appendix A-table 1
Simplified guide to the World Reference Base for Soil Resources (WRB) Reference Soil Groups (RSGs) with codes (IUSS Working Group WRB, 2022)

	RSG	Code
1. Soils with thick organic layers:	Histosols	HS
2. Soils with strong human influence –		
With long and intensive agricultural use:	Anthrosols	AT
Containing significant amounts of artefacts:	Technosols	TC
3. Soils with limitations to root growth		
Permafrost-affected:	Cryosols	CR
Thin or with many coarse fragments:	Leptosols	LP
With a high content of exchangeable Na:	Solonetz	SN
Alternating wet-dry conditions, shrink-swell clay minerals:	Vertisols	VR
High concentration of soluble salts:	Solonchaks	SC
4. Soils distinguished by Fe/Al chemistry		
Groundwater-affected, underwater or in tidal areas:	Gleysols	GL
Allophanes and/or Al-humus complexes:	Andosols	AN
Subsoil accumulation of humus and/or oxides:	Podzols	PZ
Accumulation and redistribution of Fe:	Plinthosols	PT

(*continued on next page*)

Appendix A-table 1 (*continued*)

	RSG	Code
Stagnant water, abrupt textural difference:	Planosols	PL
Stagnant water, structural difference and/or moderate textural difference:	Stagnosols	ST
Low-activity clays, P fixation, many Fe oxides, strongly structured:	Nitisols	NT
Dominance of kaolinite and oxides:	Ferralsols	FR
5. Pronounced accumulation of organic matter in the mineral topsoil		
Very dark topsoil, secondary carbonates:	Chernozems	CH
Dark topsoil, secondary carbonates:	Kastanozems	KS
Dark topsoil, no secondary carbonates (unless very deep), high base status:	Phaeozems	PH
Dark topsoil, low base status:	Umbrisols	UM
6. Accumulation of moderately soluble salts or non-saline substances		
Accumulation of, and cementation by, secondary silica:	Durisols	DU
Accumulation of secondary gypsum:	Gypsisols	GY
Accumulation of secondary carbonates:	Calcisols	CL
7. Soils with clay-enriched subsoil		
Interfingering of coarser-textured, lighter-coloured material into a finer-textured, stronger coloured layer:	Retisols	RT
Low-activity clays, low base status:	Acrisols	AC
Low-activity clays, high base status:	Lixisols	LX
High-activity clays, low base status:	Alisols	AL
High-activity clays, high base status:	Luvisols	LV
8. Soils with little or no profile differentiation		
Moderately developed:	Cambisols	CM
Stratified fluviatile, marine or lacustrine sediments:	Fluvisols	FL
Sandy:	Arenosols	AR
No significant profile development:	Regosols	RG

Appendix A-

Table 2Soil and water conservation engineering measures factor (E) assignment table.

Secondary Category	Name of Engineering Measures	Engineering Measure Code	E-Factor Value
Stepped fields	Earthen-paved terraced fields	20101	0.084
	Stone-paved terraced fields	20102	0.121
	Terraced fields on slopes	20103	0.414
	Terraced fields on cross-slope	20104	0.347
Embankment or foothpath between paddy fields	-	202	0.347
Horizontal steps (reverse slope terraces)	-	204	0.151
Horizontal groove	-	205	0.335
Fish scales pit	-	206	0.249
Large fruit tree pits	-	207	0.160
Non-engineering measures	-	-	**1.000**

Note: In addition to the above soil and water conservation engineering measures need to be assigned a factor value, other measures are only statistical area, length or number of places, not assigned a factor value, and not included in the calculation of the soil erosion model, i.e., the E factor is assigned a value of 1.

Appendix A-

Table 3Assignment of Tillage Measure Factor T (Appendix: 70 Years of Farming Systems in China).

First class area	First class district name	Secondary area	Secondary district names	T-factor value
01	Cool-loving crops of the Qinghai-Tibetan Plateau with one-ripening rotational zone	11	The cool-loving, first-maturing zone in the western Sichuan valley of south-eastern Tibet.	0.272
		12	Cool-loving crops of the Haibei Gannan Plateau in the first-ripening rotation area	0.272
02	Northern Central Plateau Semi-Arid Cool-Friendly Crops First Maturity Zone (NCMP)	21	The mountainous, semi-arid, cool-loving, first-maturing area of the Jinbei Plateau in the Houshan dams	0.488
		22	Longzhongqingdongningzhongnan loess hilly semi-arid cool-loving crop first maturity area	0.488
03	Northern Low Plateau Early Preferred Temperate Maturity Zone (NLPE)	31	Semi-arid thermophilic crops of the first maturity zone in Liaoji, Ximeng, Southeast China and North China.	0.417
		32	Drought-prone and temperature-loving crops in the eastern Loess Plateau, a hot zone	0.417
		33	Semi-moist, drought-prone, first-maturity crop filling area in eastern Jindong.	0.417
		34	Semi-moist and drought-prone winter wheat and first-maturing landfill areas in the north of China and east of China	0.417
04	Northeast Plain Hills Semi-Humid Temperate Crops First Maturity Zone	41	Large and small Xing'anling foothills and granite areas with cooler crops in the first maturity zone	0.331

(*continued on next page*)

Appendix A- (*continued*)

First class area	First class district name	Secondary area	Secondary district names	T-factor value
		42	Temperate and cool-crop first-maturity zone in the Changbai Mountains of the Sanjiang Plain	0.331
		43	The Songnen Plain Temperate Crops First Maturity Area (TCPA)	0.331
		44	Liaohe Plain Hills Warm Crop First Maturity Reclamation Area	0.331
05	Arid north-west irrigated monoculture and dichotomous zone	51	West of the Loop Irrigated First Mature Reclamation Area	0.279
		52	Irrigated one-maturity reclamation area in the northern border	0.281
		53	East Xinjiang Oasis of South Xinjiang, second maturity and first maturity area	0.281
06	Yellow-Huaihai Plain Hilly Water-consumed Land Two-maturing and Early Land Two-maturing and One-maturing Zones	61	Yanshan-Taishan premontane plains water-sourced land set with double maturity and early maturity area.	0.397
		62	Heilonggang water-scarce low plains irrigated land two-maturing and early-maturing zone	0.426
		63	Grain and Cotton Two-Maturing and One-Maturing Zones in the Low Plains of Northwest Lu and North Henan Province	0.391
		64	Peanut and Cotton One-Maturity Area on Dry Slopes of Water-consumed Land in the Hills of Shandong Province	0.425
		65	Second maturity zone of dryland watered land in the Nanyang Basin of the Huanghuai Plain	0.413
		66	Fen-Wei valley watered land two-maturing dryland one-maturing two-maturing zone	0.378
		67	Hilly mountainous dryland slopes in western Henan Province, one-maturing and two-maturing areas of watered land.	0.392
07	South-west Central Plateau mountainous dryland two-maturing and one-maturing paddy two-maturing zones	71	Qinba mountainous area of dry land with two maturing zones and two maturing zones of paddy land.	0.403
		72	Sichuan, Hubei, Hunan and Guizhou low plateau mountainous rice paddy dryland double-ripening and single-ripening area	0.396
		73	Two-maturing and one-ripening zones in dryland paddy fields on the Guizhou Plateau	0.410
		74	Yunnan Plateau Paddy Dryland Two-ripening and One-ripening Zones	0.425
		75	Yunnan-Guizhou border plateau, mountain and river valleys, early-ripening and double-ripening areas.	0.429
08	JAC Plain Hilly Wheat-Rice Bifurcation Zone (JHWRZ)	81	JAC Plain Wheat-Rice Double-Maturing and Early-Triple-Maturing Area	0.392
		82	Early-maturing and early-three-maturing areas of paddy fields in the hilly plains of EYWAN.	0.372
09	Sichuan Basin water-dry double- and triple-ripening areas	91	Two-maturing area of wheat and rice in paddy fields of Chengdu Plain, West Basin	0.422
		92	Bundung Hills Low Mountain Shui Tian Dryland Double- and Triple-maturing Area	0.411
10	Lower and middle reaches of the Yangtze River, plains and hills, paddy fields, three-maturing and two-maturing areas	101	Early third maturity and second maturity zone of hilly paddy fields along the river plains	0.338
		102	Three-maturing and two-maturing zones in the hilly paddy fields of the Two Lakes Plain	0.312
11	South-eastern hilly and mountainous paddy fields, early-maturing two-maturing three-maturing zone	111	Zhejiang and Fujian hilly and mountainous paddy and dryland triple maturity and double maturity areas	0.354
		112	Nanling hilly mountainous paddy dryland bi-maturity and tri-maturity areas	0.338
		113	Dryland paddy fields with double and triple maturity areas in the mountainous areas of south Yunnan Province	0.395
12	**South China Hilly Coastal Plain Late-Triple-Maturing and Hot-Triple-Maturing Zones**	**121**	**Late ripening area of the South China Low Hills Plain**	**0.466**
		122	South China Coastal Xishuangbanna Tainan Second and Third Maturity and Hot Crop Zone	0.459

Note: For details of the national crop rotation zones, see appendix 3 of 70 Years of China's Tillage System, a list of counties (cities) in China's tillage system (China Agricultural Publishing House, 2005).

Appendix A-Figure 1. Random monitoring sites for validation samples (pictures of some highly eroded areas)

References

[1] J.L. Li, J.H. Chen, L. Hua, Space and temporal changes of soil erosion in Hubei province based on CSLE, J. Soil Water Conserv. 36 (4) (2022) 43–52.
[2] C.H. Zhou, W.M. Cheng, J.K. Q, 1:1 million digital geomorphology classification system research, Journal of Earth Information Science 11 (6) (2009) 707–724.
[3] D. Pimentel, Soil erosion: a food and environmental threat, Environ. Dev. Sustain. 8 (2006) 119–137.
[4] R. Lal, W.C. Moldenhauer, Effects of soil erosion on crop productivity, Crit. Rev. Plant Sci. 5 (4) (1987) 303–367.
[5] D. Pimentel, N. Kounang, Ecology of soil erosion in ecosystems, Ecosystems 1 (1998) 416–426.
[6] M. José, R. García, The effects of land uses on soil erosion in Spain: a review, Catena 81 (1) (2010) 1–11.
[7] P. Borrelli, D.A. Robinson, L.R. Fleischer, An assessment of the global impact of 21st century land use change on soil erosion, Nat. Commun. 8 (1) (2017) 1–13.
[8] F.G.A. Verheijen, R.J.A. Jones, R.J. Rickson, Tolerable versus actual soil erosion rates in Europe, Earth Sci. Rev. 94 (1–4) (2009) 23–38.
[9] R. Benavidez, B. Jackson, D. Maxwell, A review of the (Revised) Universal Soil Loss Equation ((R) USLE): with a view to increasing its global applicability and improving soil loss estimates, Hydrol. Earth Syst. Sci. 22 (11) (2018) 6059–6086.
[10] S.D. Angima, D.E. Stott, M.K. O'neill, Soil erosion prediction using RUSLE for central Kenyan highland conditions, Agric. Ecosyst. Environ. 97 (1–3) (2003) 295–308.
[11] J.M. Laflen, W.J. Elliot, D.C. Flanagan, WEPP-predicting water erosion using a process-based model, J. Soil Water Conserv. 52 (2) (1997) 96–102.
[12] I. Takken, L. Beuselinck, J. Nachtergaele, Spatial evaluation of a physically-based distributed erosion model (LISEM), Catena 37 (3–4) (1999) 431–447.
[13] A. Pandey, V.M. Chowdary, B.C. Mal, Identification of critical erosion prone areas in the small agricultural watershed using USLE, GIS and remote sensing, Water Resour. Manag. 21 (2007) 729–746.
[14] P.P. Dabral, N. Baithuri, A. Pandey, Soil erosion assessment in a hilly catchment of North Eastern India using USLE, GIS and remote sensing, Water Resour. Manag. 22 (2008) 1783–1798.
[15] B.P. Ganasri, H. Ramesh, Assessment of soil erosion by RUSLE model using remote sensing and GIS-A case study of Nethravathi Basin, Geosci. Front. 7 (6) (2016) 953–961.
[16] S. Dun, J.Q. Wu, W.J. Elliot, Adapting the water erosion prediction project (WEPP) model for forest applications, J. Hydrol. 366 (1–4) (2009) 46–54.
[17] E. Amore, C. Modica, M.A. Nearing, Scale effect in USLE and WEPP application for soil erosion computation from three Sicilian basins, J. Hydrol. 293 (1–4) (2004) 100–114.
[18] B. Grum, K. Woldearegay, R. Hessel, Assessing the effect of water harvesting techniques on event-based hydrological responses and sediment yield at a catchment scale in northern Ethiopia using the Limburg Soil Erosion Model (LISEM), Catena 159 (2017) 20–34.
[19] V. Sheikh, V.E. Loon, R. Hessel, Sensitivity of LISEM predicted catchment discharge to initial soil moisture content of soil profile, J. Hydrol. 393 (3–4) (2010) 174–185.
[20] G.Q. Cai, Z.J. Yuan, Q.J. Cheng, Progress in the distributed erosion sand production model, Advances in Geography Science 3 (2006) 48–54.
[21] C.F. Cai, S. Ding, Z.H. Shi, Prediction of soil nutrient loss in a typical small watershed in the Three Gorges Reservoir area supported by GIS, J. Soil Water Conserv. (1) (2001) 9–12.
[22] Z.S. Jiang, F.L. Zheng, M. Wu, Study on the forecast model of slope water erosion in China, Sediment study (4) (2005) 1–6.
[23] B.Y. Liu, Y.N. Liu, K.L. Zhang, Classification of soil and water conservation measures in China, J. Soil Water Conserv. 27 (2) (2013) 80–84.
[24] Z.Y. Liu, W.B. Zhang, B. Yin, Spatial distribution characteristics of soil erosion intensity in the pan-third pole region based on CSLE, Res. Soil Water Conserv. 31 (3) (2024) 1–9.
[25] H.F. Zhao, Environmental evolution characteristics of typical lake deposition and watershed erosion, in: Holocene China, Northwest A&F University, 2023.
[26] Z.L. Han, Z.Z. Li, L. Zhang, Space and temporal change analysis of soil erosion in Helen City from 2000 to 2020, Land and Natural Resources Research (5) (2023) 24–30.
[27] X.Z. Pan, Y. Liang, D. Li, et al., Field calibration of soil erosion maps based on 3S integration technology, Soil (6) (2007) 948–952.
[28] Y. Liang, B. Zhang, X. Pan, et al., Trend analysis of soil erosion dynamics in the southern red soil zone, J. Soil 41 (4) (2009) 534–539.
[29] M.Y. Wang, L.C. Wang, L. Mo, Theoretical research and practice of water ecology evaluation in tropical Island basin-taking hainan Island as an example, Environmental Science in China 28 (3) (2024) 1–10.
[30] L.R. Zhu, Y.H. Liu, C.Q. Ye, Change and influencing factors of Changhua River in arid area of hainan Island, Ecological Science 39 (1) (2020) 183–189.
[31] M. Xiao, Application of GIS in Watershed Ecological Environment Quality Evaluation, Hainan University, 2011.
[32] H. Xiao, Z.Y. Ouyang, X.K. Wang, Spatial distribution characteristics of soil erosion in Hainan Island supported by GIS, Journal of Soil Erosion and Soil and Water Conservation (4) (1999) 75–80.
[33] H. Xiao, Z.Y. Ouyang, J.Z. Zhao, Assessment of spatial distribution characteristics of soil conservation and ecological economic value in Hainan ecosystem, J. Ecol. (4) (2000) 552–558.
[34] E.M. Rao, Y. Xiao, Z.Y. Ouyang, Spatial characteristics and influencing factors of soil conservation function in the ecosystem of Hainan Island, J. Ecol. 33 (3) (2013) 746–755.
[35] L. Chen, Spatio-temporal Variation Characteristics of Rainfall and Rainfall Erosion Force in Typical Red Soil Areas in Southern China, Nanjing Agricultural University, 2020.
[36] M. Xiao, J.Q. Wu, Q.B. Chen, Dynamic changes of land use in the Changhua River basin based on the CA-Markov model, Journal of Agricultural Engineering 28 (10) (2012) 231–238.
[37] W. Chen, C. Chen, L. Li, Spatiotemporal analysis of extreme hourly precipitation patterns in Hainan Island, South China, Water 7 (5) (2015) 2239–2253.
[38] X.R. Cheng, Y.M. Hu, Z.H. Liu, et al., Quantitative study of soil erosion in Guangzhou city based on remote sensing data to improve the modified generic soil loss equation, J. Soil Bulletin 54 (3) (2023) 559–568.
[39] B. Gholamahmadi, S. Jeffery, O. Gonzalez-Pelayo, et al., Biochar impacts on runoff and soil erosion by water: a systematic global scale meta-analysis, J. Science of the Total Environment 871 (2023) 161860.
[40] P. Borrelli, P. Panagos, C. Alewell, et al., Policy implications of multiple concurrent soil erosion processes in European farmland, Nat. Sustain. 6 (1) (2023) 103–112.
[41] P. Dash, S.L. Sanders, P. Parajuli, Improving the accuracy of land use and land cover classification of Landsat data in an agricultural watershed, Rem. Sens. 15 (16) (2023) 4020.
[42] M.S. Chowdhury, Comparison of accuracy and reliability of random forest, support vector machine, artificial neural network and maximum likelihood method in land use/cover classification of urban setting, Environmental Challenges 14 (2024) 100800.
[43] E. Gülher, U. Alganci, Satellite-derived bathymetry mapping on Horseshoe Island, Antarctic Peninsula, with open-source satellite images: evaluation of atmospheric correction methods and empirical models, Rem. Sens. 15 (10) (2023) 2568.
[44] C. Giacomo, S. Riccardo, Unnamed soils, lost opportunities, Environmental Science & Technology 53 (15) (2019) 8477–8478.
[45] IUSS Working Group WRB, World Reference Base for Soil Resources. International Soil Classification System for Naming Soils and Creating Legends for Soil Maps, fourth ed., International Union of Soil Sciences (IUSS), Vienna, Austria, 2022, p. 234.
[46] B.Y. Liu, S.Y. Guo, Z.G. Li, Water erosion sampling survey in China, Soil and Water Conservation in China 10 (2013) 26–34.
[47] W.B. Zhang, Y. Xie, B.Y. Liu, Research on calculating the erosion force of rainfall by using daily rainfall, Geographical Sciences (6) (2002) 705–711.
[48] Y. Xie, B.Y. Liu, W.B. Zhang, Standards study on erosion rainfall, J. Soil Water Conserv. (4) (2000) 6–11.
[49] Y. Zhang, J.P. Yuan, B.Y. Liu, Progress in studying vegetation cover and management factors in soil erosion prediction model, J. Appl. Ecol. (8) (2002) 1033–1036.
[50] H. Zhang, The CSLE model based soil erosion prediction: comparisons of sampling density and extrapolation method at the county level, Catena 165 (2018) 465–472.51.

[51] Y.Q. Zhu, Z.B. Zhao, G.P. Qi, The estimation model of secondary precipitation erosion force based on precipitation characteristics-takes the typical small watershed in the loess hilly and gully region as an example, Journal of Irrigation and Drainage 42 (11) (2023) 98–105.
[52] J.Z. Zhang, S.H. Mo, K.X. Jiang, Spatio-temporal evolution characteristics of rainfall erosion force in Jialing River Basin based on model applicability analysis, J. Xi'an Univ. Technol. 28 (3) (2024) 1–9.
[53] Q.M. Zhu, N. Wang, J.E. Liu, Soil water erosion change and driving factor in ecologically fragile areas of northern Shaanxi-Take Yulin city as an example, Res. Soil Water Conserv. 30 (5) (2023) 41–51.
[54] S.F. Wu, B. Zhang, X.J. Shi, Z.Y. Yuan, H. Feng, The FLUS-CSLE model predicts soil erosion in different land-use change scenarios in typical watersheds of the Loess Plateau, Journal of Agricultural Engineering 38 (24) (2022) 83–92.
[55] P.I.A. Kinnell, AGNPS-UM: applying the USLE-M within the agricultural non point source pollution model, Environ. Model. Software 15 (3) (2000) 331–341.
[56] A. Pandey, V.M. Chowdary, B.C. Mal, Identification of critical erosion prone areas in the small agricultural watershed using USLE, GIS and remote sensing, Water Resour. Manag. 21 (2007) 729–746.
[57] H. Zhang, Q. Yang, R. Li, Extension of a GIS procedure for calculating the RUSLE equation LS factor, Comput. Geosci. 52 (2013) 177–188.
[58] H. Zhang, J. Wei, Q. Yang, An improved method for calculating slope length (λ) and the LS parameters of the Revised Universal Soil Loss Equation for large watersheds, Geoderma 308 (2017) 36–45.
[59] Y. Zou, Y. Wang, Y. He, Soil erosion characteristics in tropical Island watersheds based on CSLE model: discussion of driving mechanisms, Land 13 (3) (2024) 302.
[60] W. Shi, M. Huang, S.L. Barbour, Storm-based CSLE that incorporates the estimated runoff for soil loss prediction on the Chinese Loess Plateau, Soil Tillage Res. 180 (2018) 137–147.
[61] X. Duan, Z. Bai, L. Rong, Investigation method for regional soil erosion based on the Chinese Soil Loss Equation and high-resolution spatial data: case study on the mountainous Yunnan Province, China, Catena 184 (2020) 104237.
[62] D. Wuepper, P. Borrelli, R. Finger, Countries and the global rate of soil erosion, Nat. Sustain. 3 (1) (2020) 51–55.
[63] H. Wei, W.W. Zhao, Selection of the optimal estimation method for soil erodibility K value: a case study of ansai watershed area in northern shaanxi, Science of Soil and Water Conservation 15 (6) (2017) 52–65.
[64] H. Tanyaş, Ç. Kolat, M.L. Süzen, A new approach to estimate cover-management factor of RUSLE and validation of RUSLE model in the watershed of Kartalkaya Dam, J. Hydrol. 528 (2015) 584–598.
[65] G. Wang, G. Gertner, X. Liu, Uncertainty assessment of soil erodibility factor for revised universal soil loss equation, Catena 46 (1) (2001) 1–14.
[66] K.L. Zhang, A.P. Shu, X.L. Xu, Soil erodibility and its estimation for agricultural soils in China, J. Arid Environ. 72 (6) (2008) 1002–1011.
[67] Z. Song, Y. Lu, Z. Ding, A new remote sensing desert vegetation detection index, Rem. Sens. 15 (24) (2023) 5742.
[68] Y. Wang, L.N. Hao, Q. Xu, Analysis of the spatial and temporal evolution characteristics and geographical factors of vegetation cover in the Loess Plateau from 2001 to 2019, J. Ecol. 43 (6) (2023) 11.
[69] Z. Jiang, A.R. Huete, J. Chen, Analysis of NDVI and scaled difference vegetation index retrievals of vegetation fraction, Remote sensing of environment 101 (3) (2006) 366–378.
[70] B. Zhang, Z. Chen, X. Shi, Analysis of temporal and spatial changes of soil erosion under LULCC based on CSLE in the typical watershed on the Loess Plateau, Authorea Preprints (2022).
[71] D. Li, Y. Ping, Analysis of the influence of rainfall infiltration condition on slope stability, Shanxi Architecture 48 (12) (2022) 74–77.
[72] Y.X. Chen, Q.K. Yang, B.Y. Liu, Evaluation of soil erosion intensity in the Pearl River Basin based on the CSLE model. Chinese water and soil conservation, Science (Chinese and English) 19 (6) (2021) 86–93.
[73] Q.K. Guo, B.Y. Liu, S.B. Zhu, Main soil and water conservation tillage measure factors in China, Soil and Water Conservation in China 10 (2013) 5.
[74] B.F. Yuan, H.F. Cui, M. Li, The influence of different soil and water conservation measures on slope farmland in northeast China, Soil and Water Conservation in China 2 (2024) 61–65.
[75] S. Li, J. Kang, J. Ye, Analysis of soil erosion changes and influencing factors based on the CSLE model and GeoDector in Dongjiang River Basin of China, Soil Sci. Soc. Am. J. 88 (3) (2024) 718–729.
[76] X. Xie, C. Li, L. Wu, Improvement of land surface vegetation ecology inhibited precipitation-triggered soil erosion in the alpine-cold river source area–A case study in Southern Gansu, China, J. Hydrol.: Reg. Stud. 51 (2024) 101614.
[77] T. Raza, M. Shehzad, M. Abbas, Impact assessment of COVID-19 global pandemic on water, environment, and humans, Environmental Advances 11 (2023) 100328.
[78] Q. Meng, J. Qian, U. Schlink, Anthropogenic heat variation during the COVID-19 pandemic control measures in four Chinese megacities, Remote Sensing of Environment 293 (2023) 113602.
[79] Z. Feng, X. Wang, J. Yuan, Changes in air pollution, land surface temperature, and urban heat islands during the COVID-19 lockdown in three Chinese urban agglomerations, Sci. Total Environ. 892 (2023) 164496.
[80] C. Wang, Design and reflection on comprehensive management measures for small watersheds in hainan, Value Eng. 39 (27) (2020) 7–8.